

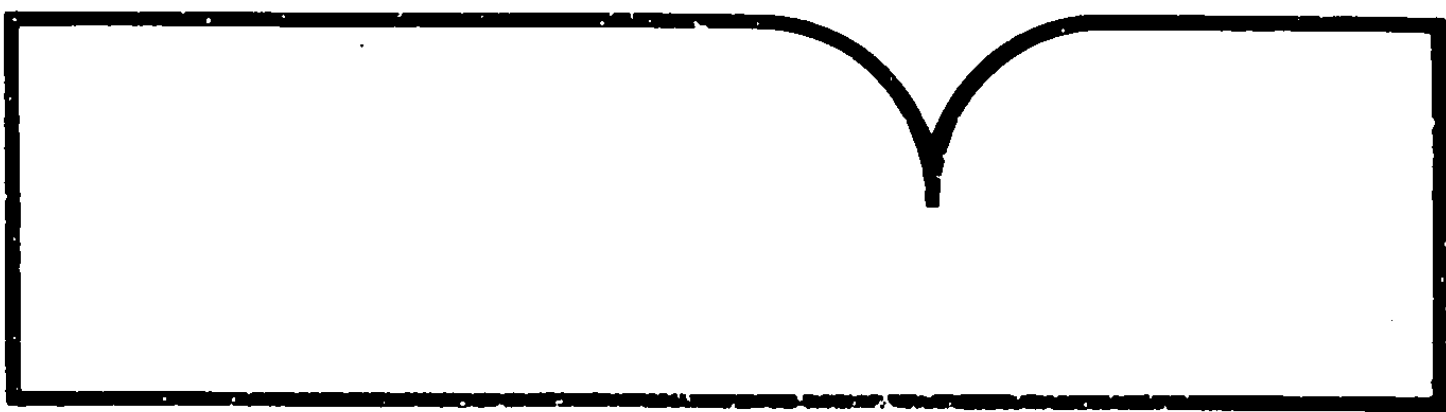
Biphase Turbine for Reverse
Osmosis Desalination

Transamerica Delaval, Inc., Santa Monica, CA

Prepared for

Office of Water Research and Technology
Washington, DC

Dec 82



BIBLIOGRAPHIC INFORMATION

PB83-255513

Biphase Turbine for Reverse Osmosis Desalination.

Dec 82

Paul L. Limburg.

PERFORMER: Transamerica Delaval, Inc., Santa Monica, CA.
Biphase Energy Systems.
Contract DI-14-34-0001-1487

SPONSOR: Office of Water Research and Technology,
Washington, DC.
WB303910 OWRTC-10121-S(1487) (1)
Final rept.

A new hydraulic reaction turbine was designed to recover the power available in the high-pressure waste-brine stream of reverse osmosis desalination systems. A reaction turbine sized for reverse-osmosis systems producing 600 gph was built and tested. The turbine performed well driving either a variable-speed pump or an electrical generator. Measured turbine efficiency (shaft power divided by available power) was 63%, compared with a prediction of 67%. The turbine can be built with larger capacity to reduce the size, weight and power consumption of reverse osmosis desalination systems. Efficiency of larger units is predicted to lie in the range of 65 to 70%.

KEYWORDS: *Hydraulic turbines, *Desalting, *Reverse osmosis desalination, *Energy recovery.

Available from the National Technical Information Service,
Springfield, Va. 22161

PRICE CODE: PC A04/MF A01

Selected Water Resources Abstracts **W 250508**

1. Report No. 2.

3. Accession No.

W 83-03910

Input Transaction Form

4. Title
BIPHASE TURBINE FOR REVERSE OSMOSIS DESALINATION,

5. Report Date

6.

8. Performing Organization Report No.

7. Author(s)
LYMBURG, P.L.

10. Project No. **DWRT
C-10121-S (#1457)(1)**

9. Organization
**Transamerica Delaval Inc.
Biphase Energy Systems,
2000 Airport Ave.
Santa Monica, CA. 90405**

11. Contract/Grant No
14-34-0001-1487 (47)

13. Type of Report and Period Covered

12. Sponsoring Organization

15. Supplementary Notes **Completion Report, December 1982.**

49 Pages, 18 Figures, 7 Tables

16. Abstract

A new hydraulic reaction turbine was designed to recover the power available in the high-pressure waste-brine stream of reverse osmosis desalination systems. A reaction turbine sized for reverse-osmosis systems producing 600 gph was built and tested. The turbine performed well driving either a variable-speed pump or an electrical generator. Measured turbine efficiency (shaft power divided by available power) was 63%, compared with a prediction of 67%. The turbine can be built with larger capacity to reduce the size, weight and power consumption of reverse osmosis desalination systems. Efficiency of larger units is predicted to lie in the range of 65 to 70%.

17a. Descriptors

Power Recovery, * Turbines, * Reverse Osmosis, Hydraulic Turbines, * Desalination, Turbine efficiency.

17c. CWRR Field & Group

18. Availability Available from the National Technical Information Service as PB **PB8 3 255513**

103 A 1080

19. Security Class. (Report)
20. Security Class. (Page)

21. No. of Pages **52**
22. Price **A04-A01**

Send to:
Water Resources Scientific Information Center
OFFICE OF WATER RESEARCH AND TECHNOLOGY
U.S. DEPARTMENT OF THE INTERIOR
Washington, D.C. 20240

Abstractor

Institution

BIPHASE TURBINE FOR REVERSE OSMOSIS DESALINATION

FINAL REPORT

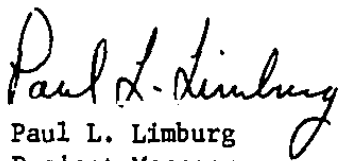
Prepared for

U.S. DEPARTMENT OF THE INTERIOR
Office of Water Research and Technology

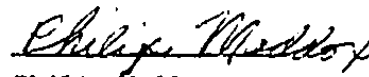
Contract No. 14-34-0001-1487

December 1982

Prepared by:


Paul L. Limburg
Project Manager

Approved by:


Philip Maddox
Technical Director

REPRODUCED BY
NATIONAL TECHNICAL
INFORMATION SERVICE
U.S. DEPARTMENT OF COMMERCE
SPRINGFIELD, VA 22161

FOREWORD

This study was sponsored by the U.S. Department of the Interior, Office of Water Research and Technology and the U.S. Army Mobility Equipment Research and Development Command at Fort Belvoir, Virginia. Mr. Melvin Lew directed the work for OWRT and Mr. G. Eskelund and Mr. Matias Santiago directed the work for MERADCOM.

At Biphase Energy Systems, Brian O'Connor, Daniel Rovner, Emil Ritzi and Makund Kavia provided design and analysis; Jack Jolley, Louis Drobnick and Chuck Dame built and tested the turbine, and Treva Meredith prepared the reports.

CONTENTS

	Page
1. Abstract	1-1
2. Summary	2-1
3. Power-Recovery Reaction Turbine	3-1
4. Test System	4-1
5. Test Results	5-1
6. Power-Recovery Turbine for Larger Systems	6-1
7. Increased Power by Waste-Brine Heating	7-1
8. Recommendations	8-1

1. ABSTRACT

A new hydraulic reaction turbine was designed to recover the power available in the high-pressure waste-brine stream of reverse osmosis desalination systems. A reaction turbine sized for reverse-osmosis systems producing 600 gph was built and tested. The turbine performed well driving either a variable-speed pump or an electrical generator. Measured turbine efficiency (shaft power divided by available power) was 63%, compared with a prediction of 67%. The turbine can be built with larger capacity to reduce the size, weight and power consumption of reverse osmosis desalination systems. Efficiency of larger units is predicted to lie in the range of 65 to 70%.

2. SUMMARY

Reverse-osmosis desalination produces a waste stream of high-pressure brine. The power in this waste-brine stream can be 70% of the total power input to the process. If this power is recovered and recycled, the input power requirements will be reduced. Additionally, space and weight reductions are possible with a smaller power source for the process.

Existing power recovery devices contain limitations. Reverse-running centrifugal pumps have low efficiency. Positive displacement expanders are susceptible to vibration and valve wear. Pelton-wheel turbines contain complex geometry and are expensive to build.

Biphase Energy Systems has built and tested a new hydraulic turbine which can recover the power in the waste-brine stream. The turbine was sized for test with the Army's Reverse Osmosis Water Purification Unit which produces 600 gph of fresh water.

This report describes the fabrication and performance testing of the first turbine and application to larger size reverse-osmosis systems. Following are the key results and conclusions.

1. A power-recovery reaction turbine for 600-gph reverse-osmosis-desalination plants was built and tested. The measured shaft power produced was 4.2 kw (5.6 hp) at the 750-psig design inlet pressure and flow of 20.7 gpm. Measured efficiency was 63% compared with the design goal of 67%. Efficiency shortfall was mainly due to lower than expected inlet-nozzle efficiency. The turbine operated successfully driving either a hydraulic-oil pump or an electrical generator. The turbine operated well mechanically throughout the tests.
2. The turbine can be applied to larger systems. A 100-gpm turbine coupled directly to a high-pressure pump runs at 3600 rpm and has a 16.5-inch diameter rotor. The turbine generates 21.6kw at 66% efficiency and reduces the pumping-power required by 35%. The turbine weighs about 200 lbs. Larger capacity turbines are feasible.

3. Heating the brine to produce more power by two-phase flow in the turbine is not effective. The heat input required is too large for a practicable turbine-power increase.
4. Long-term tests of the turbine should now be conducted to test reliability, maintainability and operation with salt-water flows.

3. POWER-RECOVERY REACTION TURBINE

TURBINE CONCEPT

The Biphase hydraulic power-recovery turbine is a reaction turbine which has the potential for high efficiency and low cost because of its simplicity. Figure 1 shows the reaction-turbine concept. High-pressure fluid flows through an inlet nozzle. This nozzle converts the pressure energy to kinetic energy. The jet of fluid, with large kinetic energy, flows into a rotor. The fluid flows through passages in the rotor to the outer diameter. Centrifugal forces accelerate the flow through the passages and out of the rotor through reaction jets. The velocity of the flow out of the reaction jet is in the opposite direction to the rotor tip velocity at the reaction jet. So, the absolute velocity and the kinetic energy of the flow leaving the rotor is low. Most of the change in kinetic energy of the flow between entering and leaving the rotor is converted to shaft power.

OPERATING CONDITIONS

The first turbine was designed for testing with a reverse-osmosis desalination unit producing 600 gph fresh water. The turbine conditions are:

	Primary Design Point	Secondary Design Point	Range
RO Unit Feedwater	Seawater	Brackish Water	
Inlet Pressure, psig	750	500	450 - 900
Flow, gpm	20	16.5	16.5 - 20

The primary design point is the best-efficiency operating condition. Concentrated seawater at 77°F is the working fluid. The outlet pressure is 0 psig. Because brackish-water-feed operation is also desired, we considered ways of insuring good efficiency with 500-psig turbine-inlet pressure. This is the secondary design point.

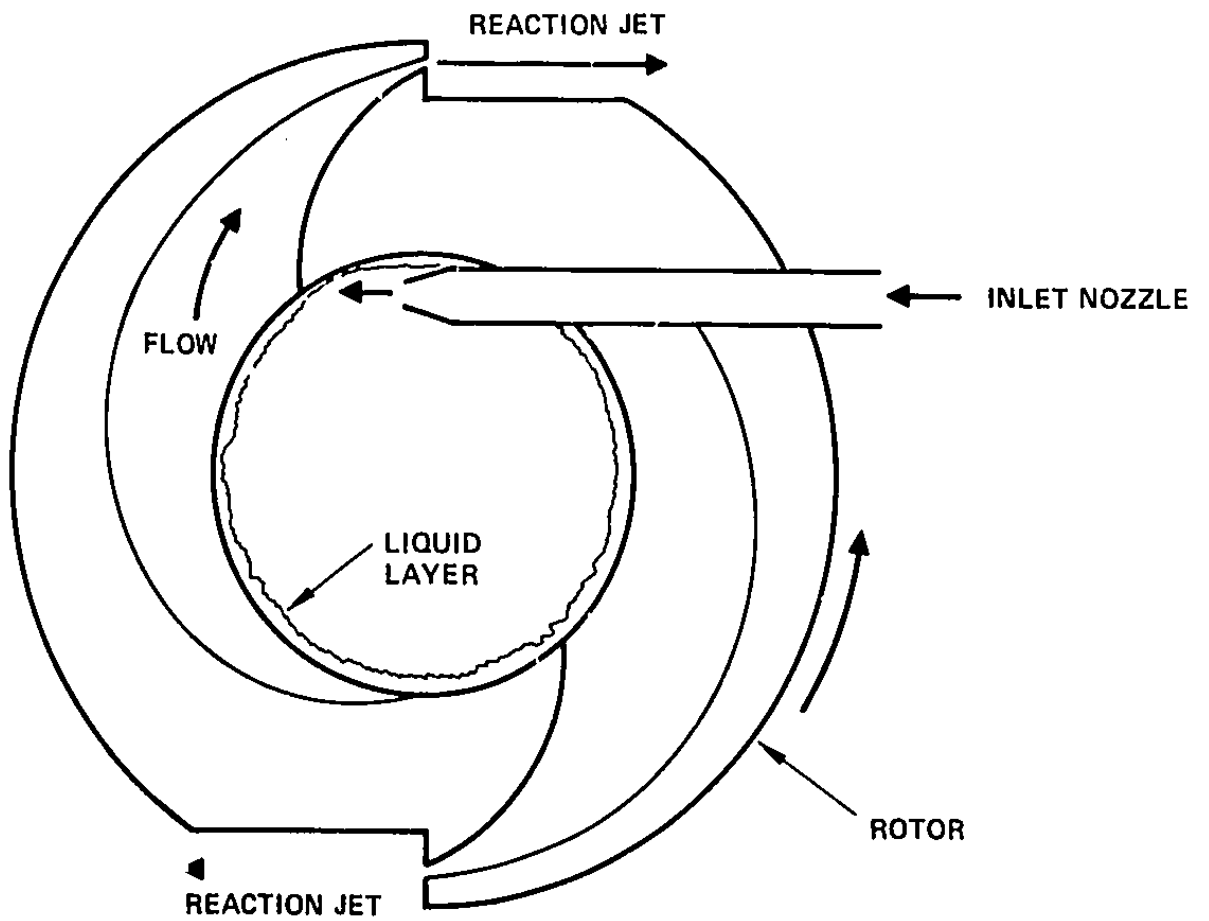


Figure 1. Reaction-Turbine Concept

PROTOTYPE TURBINE DESCRIPTION

Figure 2 shows the turbine layout. The turbine has a vertical shaft supported by two grease-lubricated ball bearings. The rotor attaches to the end of the shaft below both bearings. The inlet nozzles are on the same side of the rotor as the bearings. So, the flow enters the rotor from above. After discharge from the rotor, the flow collects in a sump below the rotor. The turbine drives an induction generator mounted on the side of the turbine housing. Figure 3 is a photograph of the turbine and generator. The turbine is made of 316L stainless steel, except for the outside legs and generator base which are carbon steel.

Upper Housing

The upper housing contains the inlet connection, inlet manifold, inlet nozzles and bearing-and-seal package.

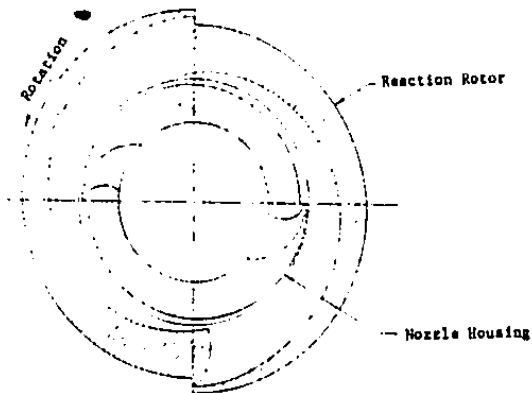
The waste-brine stream enters the turbine through a one-inch 600-lb flanged connection. The waste brine flows through an annular manifold to the inlet nozzles. There are two inlet nozzles formed by a brazed sandwich of three metal plates. The center plate is partially cut away to form the nozzle passages. The passages have a rectangular cross-section which decreases in area to 0.01 in.^2 at the nozzle exit. The inlet nozzles have a fixed size chosen for the design-point inlet pressure and flow. The inlet nozzles accelerate the flow from the inlet manifold on to the rotor.

The inlet manifold surrounds the bearing and seal package. Two ball bearings hold the turbine shaft. The grease-lubricated bearings are rugged and simple and eliminate the need for an oil pump and sump. Since the bearings contain seals, lubrication is not required after initial assembly. Two additional seals protect the bearings. At the rotor end of the shaft is a Johns-Manville Clipper Seal. At the pulley end is a Chicago Rawhide seal.

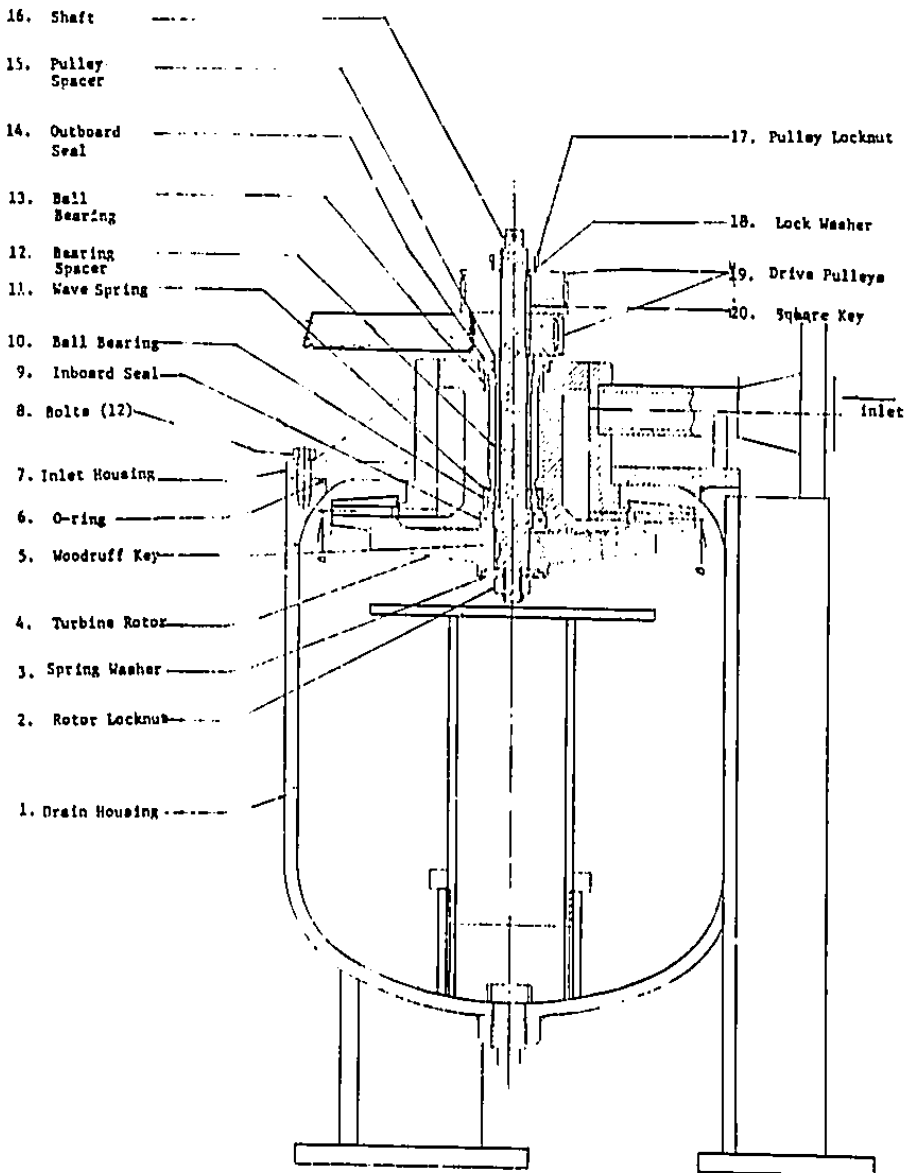
Rotor

The rotor receives the high velocity flow from the inlet nozzles. The rotor is 10.25 inches in diameter and rotates in air at 0 psig. The flow enters two passages in the rotor which lead to two reaction nozzles. Just like the inlet

A

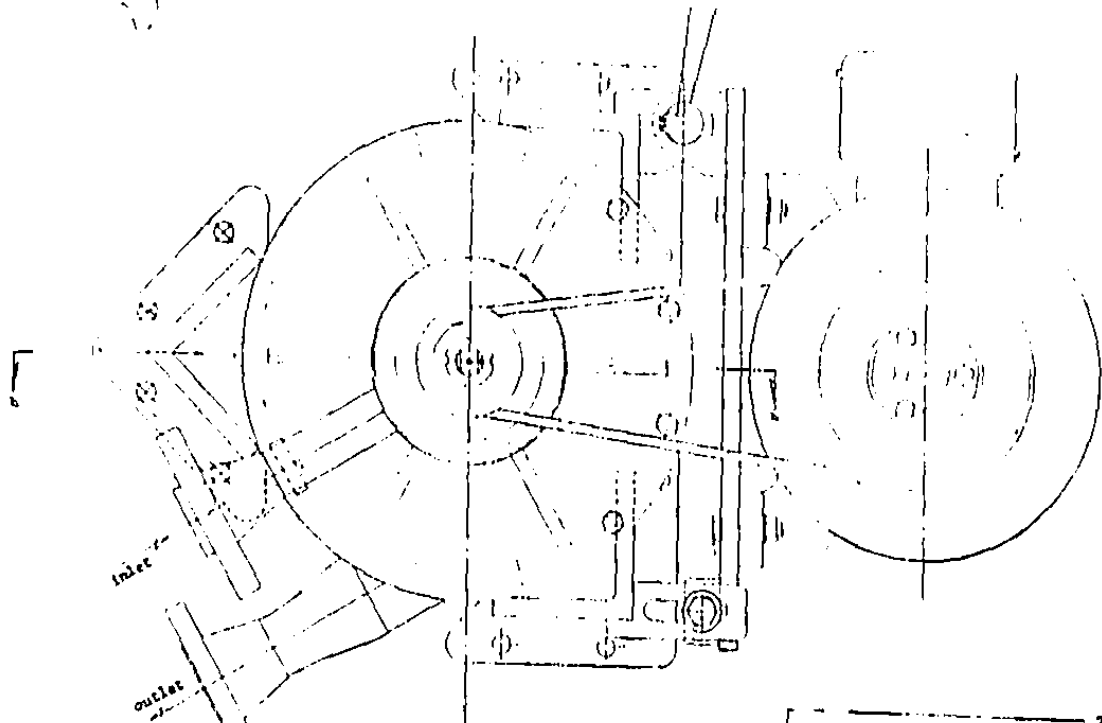


SECTION B-B

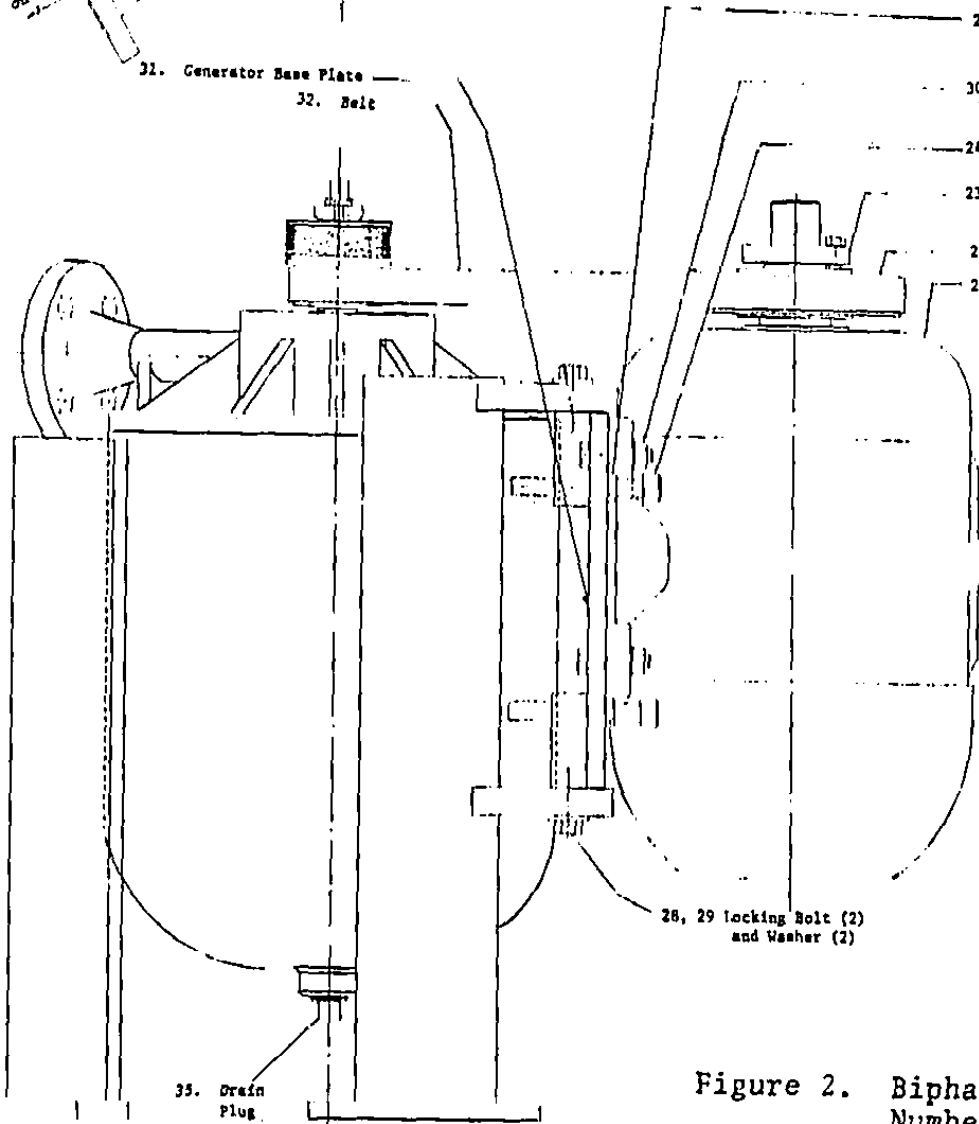


SECTION A-A





31. Generator Base Plate
32. Belt



27. Jam Nut (2)
30, 25, 26. Generator Mounting Bolt (4), Nut (4), Washer (4)
24. Tension Adjusting Bolt
23. Bushing
22. Generator Pulley
21. Generator

28, 29 Locking Bolt (2) and Washer (2)

35. Drain Plug

Figure 2. Biphase RO Hydraulic Turb Number BE-1185

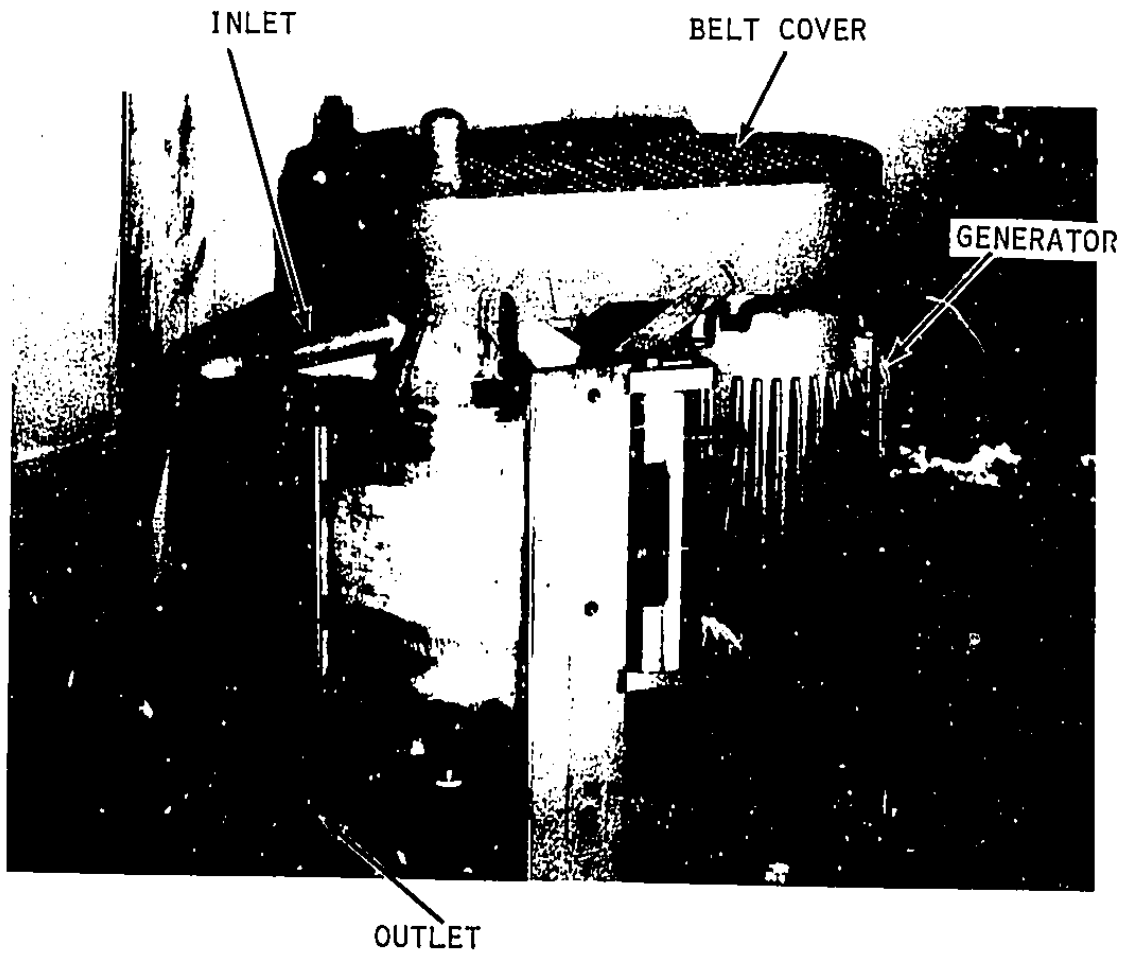


Figure 3. Power Recovery Turbine and Electrical Generator

nozzles, the rotor passages and reaction nozzles are formed by a brazed sandwich of three plates. The center plate is cut away to form the rotor passages. These passages have a rectangular cross-section which reduces to 0.11-in² at the jet exit. The passages are shaped to keep friction losses in the passages low. Figure 4 shows the rotor and shaft.

The reaction jets and rotor size are selected so that the passages are completely full at the design point conditions. If the inlet pressure decreases or the speed increases, the rotor passages will not be completely full. If the inlet pressure increases or the speed decreases, the passages overflow. The excess liquid flows over the inner rim of the rotor. The housing deflects the overflow into the sump area. The most efficient operation occurs when the passages are just completely full.

The rotor speed can be adjusted to handle lower pressure and flow conditions. By decreasing speed enough to just fill the passages, the turbine efficiency does not decrease at lower pressure operation.

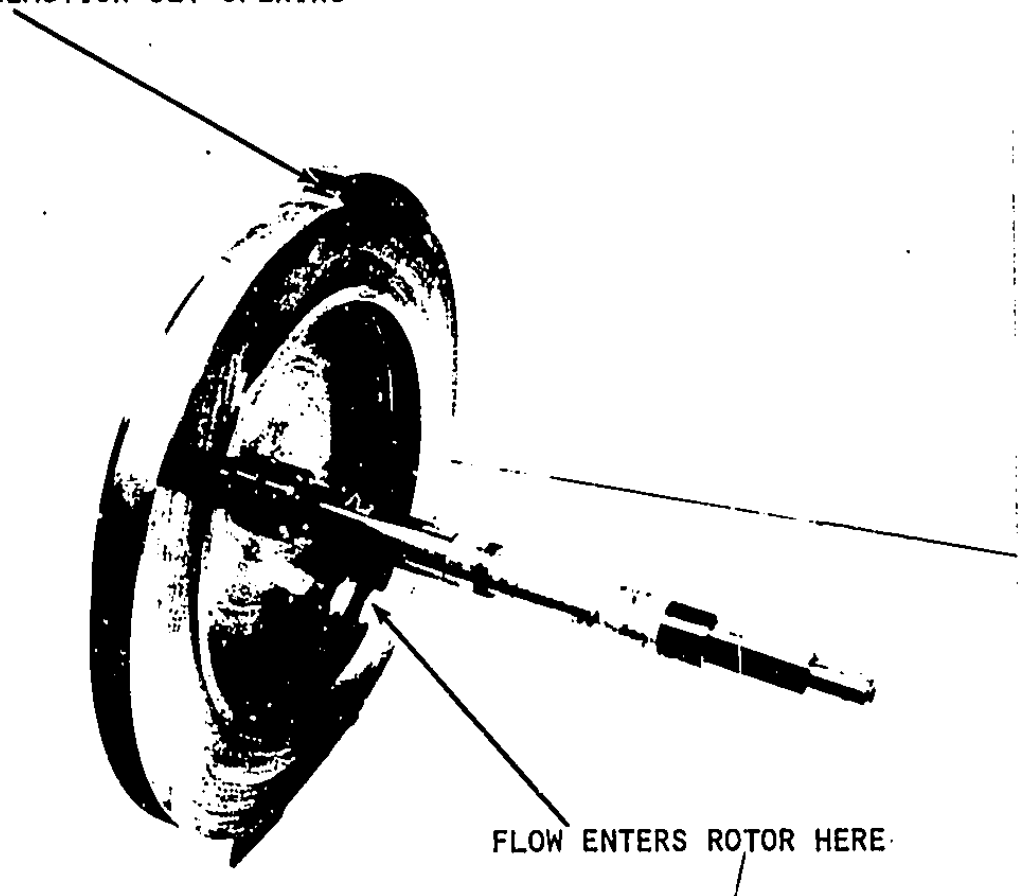
Once the reverse-osmosis process is started, the pressure and flow will not change significantly. So continuously variable speed control is not necessary. We have provided two sets of pulley drives for the generator so that the turbine can run continuously at either of two speeds. The generator speed is always the same.

The rotor housing directs the flow from the reaction jets into the sump. The flow swirls in the sump until baffles direct the flow out of the housing through a 1.5-inch flange.

Generator

The turbine drives a 7.5-hp induction generator through a belt. The generator operates at a nearly constant 3650 rpm and regulates the speed of the turbine. The generator shaft has a 6-inch pulley which can shift between two positions. The turbine output shaft has two pulleys for two operating speeds. A 2.5-inch pulley is for

REACTION JET OPENING



FLOW ENTERS ROTOR HERE

Figure 4. Turbine Rotor and Shaft

8760-rpm operation (design-point 750-psig inlet pressure) and a 3.0-inch pulley is for 7260-rpm operation (500-psig inlet pressure). The turbine can operate at either speed for a range of inlet pressures (450-900 psi). But 8760 rpm gives best efficiency with 750-psig inlet pressure and 7260 rpm gives best efficiency with 500-psig inlet pressure.

The RO plant operator will adjust the belt to the smaller pulley (8760 rpm) for operation with seawater feed and to the larger pulley (7260 rpm) for brackish-water feed. The generator is mounted on a hinged plate. Changing the hinge angle with an adjustment bolt changes the belt tension.

TURBINE PERFORMANCE PREDICTION AND DESIGN

Our analytical estimates of turbine performance are based on the following key assumptions:

1. Inlet-nozzle efficiency (nozzle-exit kinetic energy divided by isentropic energy drop through the nozzle). We assume 95% nozzle efficiency based on pipe friction data.
2. Reaction-nozzle velocity ratio (reaction-jet relative velocity divided by isentropic velocity). Again, from calculations based on pipe friction data, a velocity ratio of 0.975 is reasonable.
3. Angle of inlet jet relative to the rotor inlet. This specifies losses in the transition of flow from the inlet nozzles to the rotor. The angle is a function of the rotor inner diameter, inlet nozzle size, and the clearance between the rotor and nozzles. Increasing the rotor inner diameter or decreasing the nozzle size gives a better (smaller) inlet angle with less losses.
4. Windage, bearing and seal losses. These are a function of the speed and size of the rotor and shaft. These losses were calculated from standard correlations.

Using these assumptions, the turbine efficiency and speed is a function of the rotor size and geometry. We specified two inlet nozzles and two reaction jets

for simplicity. The efficiency increases with rotor size. However, larger rotors are heavier, harder to build and more costly. We chose a 10-inch diameter turbine as compromise. The exact turbine speed was determined by the available pulley ratios for the connection with the fixed-speed generator. The result was design-point efficiency of 67%. Turbine shaft-power output at design point is 5.9 hp. Performance predictions are presented for comparison with test results in Section 5.

TURBINE FABRICATION

Fabrication and assembly of the prototype turbine proceeded without problem except for the brazing together of the inlet-nozzle housing (part #7 in Figure 2). Figure 4A shows the inlet-nozzle braze assembly. The inlet-nozzle passages are cut out of a 0.200-inch thick plate which is brazed between two parts of the inlet housing. During the first brazing attempt, a too-long dowel-pin prevented the parts from coming together. A 0.010 gap developed in the braze joint on either side of the nozzle plate. The dowel pins align the parts during brazing and strengthen the joint afterwards.

To eliminate the gap, the nozzle plate had to be machined away. We built a new nozzle plate, cover ring and dowel pins. Then we made sure the parts fitted together securely when they entered the braze furnace. With this precaution, the braze material successfully joined the parts together without trouble.

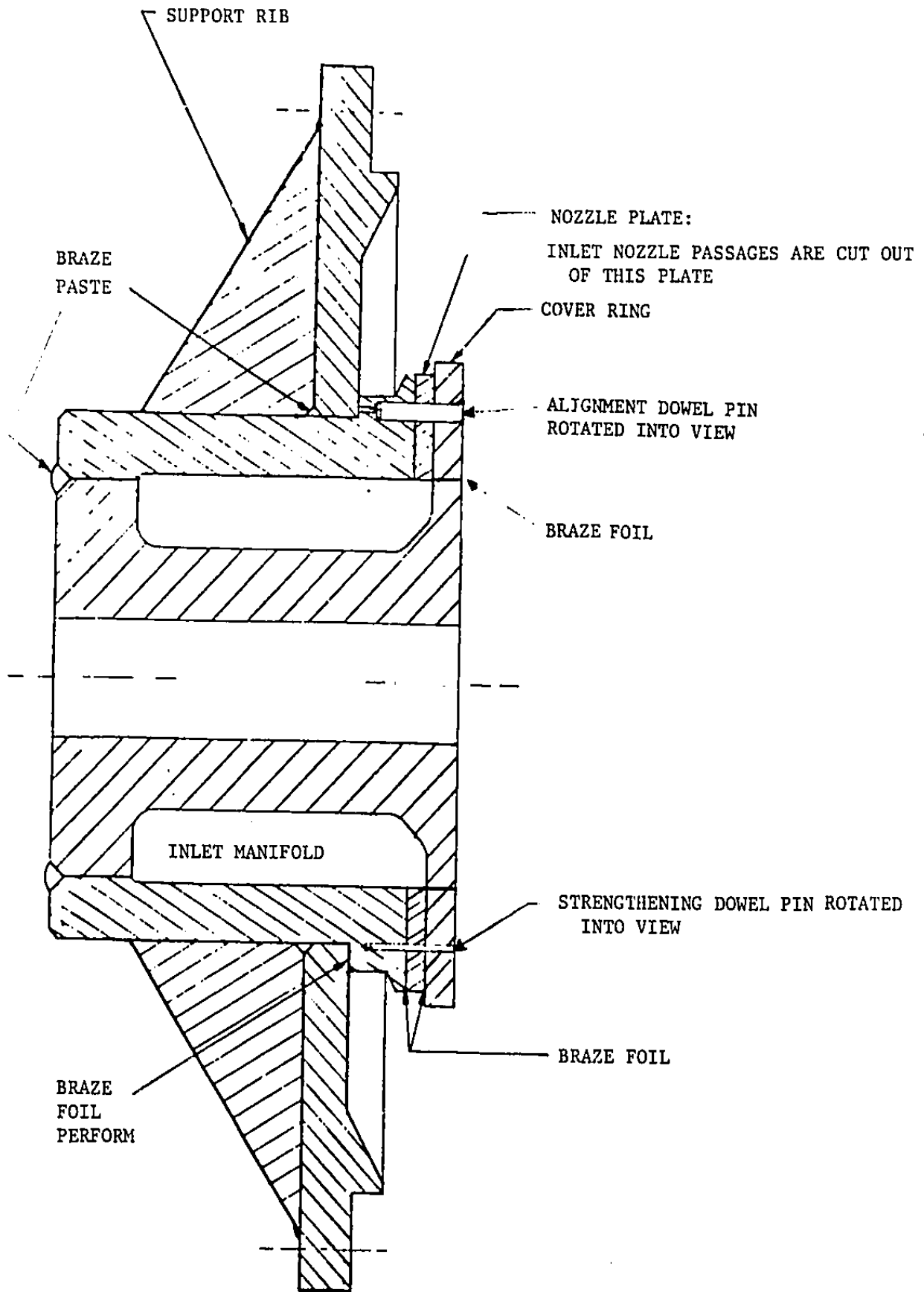


Figure 4A. Inlet-Nozzle Braze Assembly

4. TEST SYSTEM

The test system for the turbine contained the following main parts:

1. Variable-pressure (0-1000 psig) fresh-water supply.
2. Turbine with speed, torque and vibration instruments.
3. Variable-speed hydraulic-pump load.
4. Constant-speed induction-generator load.

Figure 5 is a schematic of the system.

The high-pressure water supply provided a measured and controlled flow of fresh water to the turbine. The flow simulates the waste-brine flow from a reverse-osmosis plant. The water flowed from a reservoir, through a boost pump and filter, to a 1000-psi 25-gpm positive-displacement pump. A flow orifice and pressure gage measured the flow. The pressure and flow rate were controlled by a needle valve and bypass line which returned some of the flow back to the high-pressure pump inlet.

The hydraulic turbine test system included speed and vibration instruments. A 60-tooth gear on the turbine shaft provided a speed signal to a digital tachometer. Vibration-velocity probes were mounted on the upper inlet housing to measure axial and radial vibrations.

The turbine load was either a constant-speed generator or a variable-speed hydraulic pump. The variable-speed load was used for detailed design-point and off-design performance measurements. The hydraulic-pump circulated oil through a load valve and cooler and back to an oil tank. The load valve varied the flow resistance which the hydraulic-pump had to overcome. Adjustment of the load valve provided precise control of the load on the turbine and the turbine speed.

A torque transducer measured the torque delivered by the turbine to the hydraulic pump. We then calculated turbine power from the measured torque and turbine speed.

TEST SYSTEM FOR REVERSE-OSMOSIS HYDRAULIC TURBINE

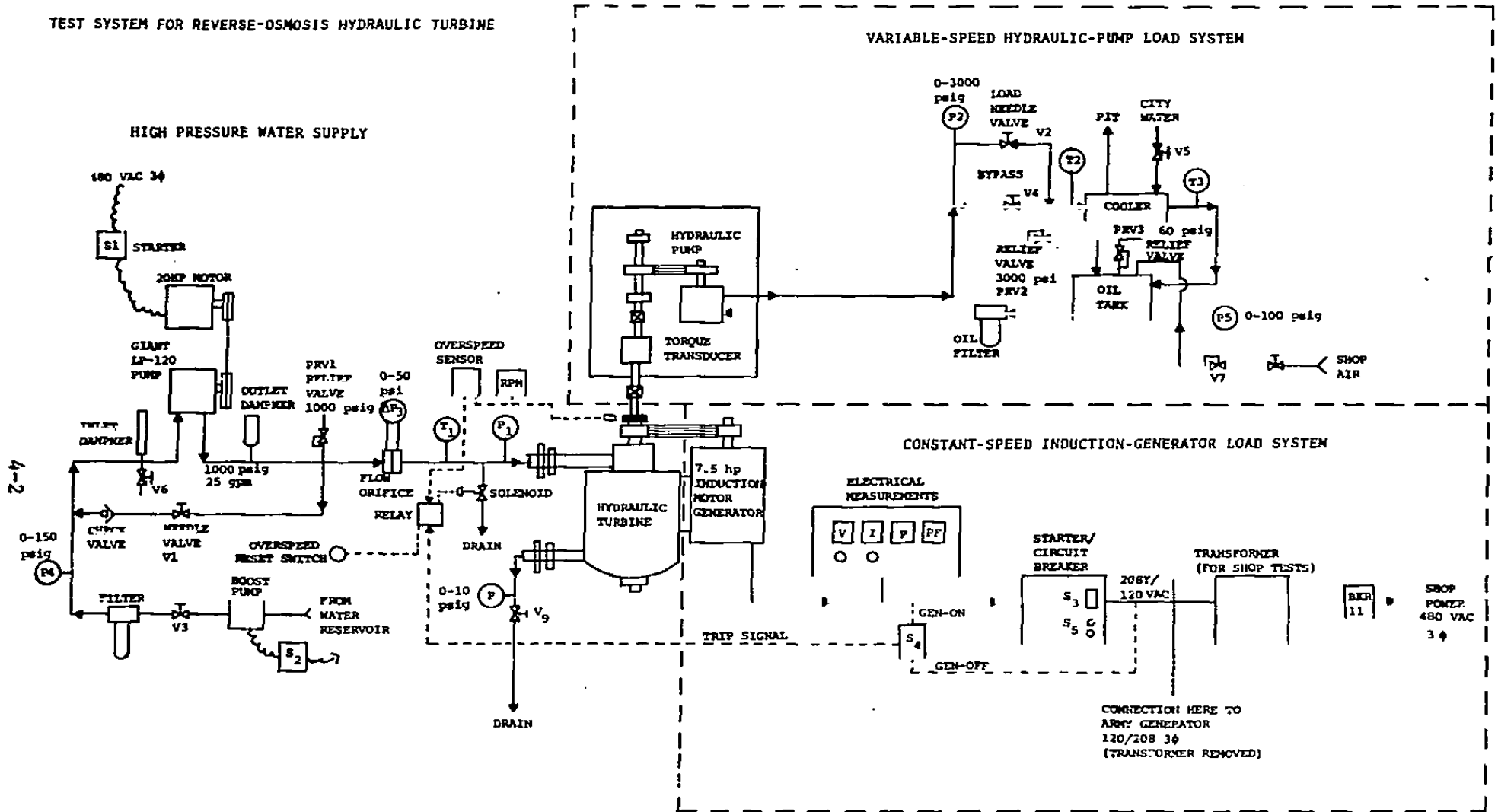


Figure 5. Test System Schematic

The constant-speed induction-generator load simulates a possible method for returning recovered power back to the reverse-osmosis system. The turbine drives the generator which makes electrical power. This power can be fed back into the electrical network of the reverse-osmosis system to help drive the high-pressure-pump motor. The induction generator we tested was designed to be compatible for tests with the Army 600-gph ROWPU system. For tests at Biphase, the power was fed through a transformer into our laboratory power system.

The induction generator runs at a nearly constant speed, just over the synchronous speed set by the frequency of the power system to which the generator is connected. The generator we used was a 7.5-hp induction motor-generator running at about 3600 rpm at 60 Hz. The generator was connected by a belt and pulleys to the turbine. The pulleys could be changed to different diameters to allow the turbine to run at certain speeds between 6900 and 9200 rpm. Also a metering panel provided approximate measurement of the generator electrical outputs: voltage, current, power and power factor.

As a safety measure, the test system also included an over-speed protection sensor. If the turbine speed became greater than a set point, or if the generator circuit breaker tripped, the sensor diverted the water flow away from the turbine inlet.

5. TEST RESULTS

SUMMARY OF TESTS

The tests to evaluate the turbine performance included the following:

1. Inlet nozzle tests. The inlet housing and nozzle was proof-tested to 1000 psig inlet pressure. Measured inlet nozzle efficiency was 87% \pm 10% compared with design goal of 95%.
2. Rotor over-speed tests. The turbine rotor was spun to 11640 rpm inside the dry turbine housing to verify mechanical integrity. This speed is just above the turbine's runaway-speed at the 750 psig design inlet pressure.
3. Variable-speed performance tests. We measured the turbine torque and power output as a function of speed. Measured efficiency at the 750-psig design inlet pressure was 62.7%. The design-goal efficiency was 67%.
4. Test with induction-generator load. The turbine drove a constant-speed induction generator and successfully produced electrical power.
5. Start-Stop test. We tested starting of the turbine-generator in two ways: first by using the turbine, and second by using the generator, to bring the turbine-generator combination up to speed. Both methods worked well. Shut-down also worked smoothly.
6. Spin-down test. The windage and bearing power was measured during a no-load spin-down of the rotor in a dry housing. At 8760 rpm design speed, measured windage and bearing power agreed with a calculated prediction of .44 hp.

INLET NOZZLE TESTS

The inlet nozzles create a high velocity jet of liquid which is directed at the inner diameter of the rotor. The turbine has two inlet nozzles. The nozzles have a rectangular cross-section with a decreasing area. The exit of the nozzle

is about .05-inch x .200-inch and has a short straight constant-area section to straighten the nozzle flow. We tested the nozzles with a straight section .100-inch long and then again with the straight section cut back to .20-inch long. The straight section provides a more columnar jet, but with the penalty of more friction loss in the nozzle.

We removed the inlet-nozzle housing from the turbine-housing and rotor in order to observe the nozzle flow. Figure 6 shows the two water jets coming from the inlet-nozzles.

Figure 7 shows the measured flow from both nozzles as a function of the inlet pressure. Because the flow through the turbine only depends on the inlet nozzles, Figure 7 also represents the turbine flowrate as a function of inlet pressure.

The nozzle efficiency η_N can be calculated from measurements of the inlet pressure, flow and nozzle-exit area:

$$\eta_N = \frac{\text{exit kinetic energy}}{\text{isentropic kinetic energy}} = \frac{\rho Q^2}{2 (P_1 - P_2) A_e^2 C_1}$$

- where
- ρ = liquid density, lbm/ft³
 - Q = volume flowrate, gpm
 - P_1, P_2 = inlet, outlet pressure, psi
 - A_e = exit area
 - C_1 = units conversion = 45,000

At 750 psig inlet pressure the nozzle efficiency was 85% \pm 10% for the longer nozzles and 87% \pm 10% for the shorter nozzles. Most of the efficiency uncertainty is due to the uncertainty (\pm 4%) of the exit-area measurement. Shortening the nozzle did improve the efficiency. The improvement was confirmed by increased turbine-efficiency measurements described below.

Reproduced from
best available copy. 

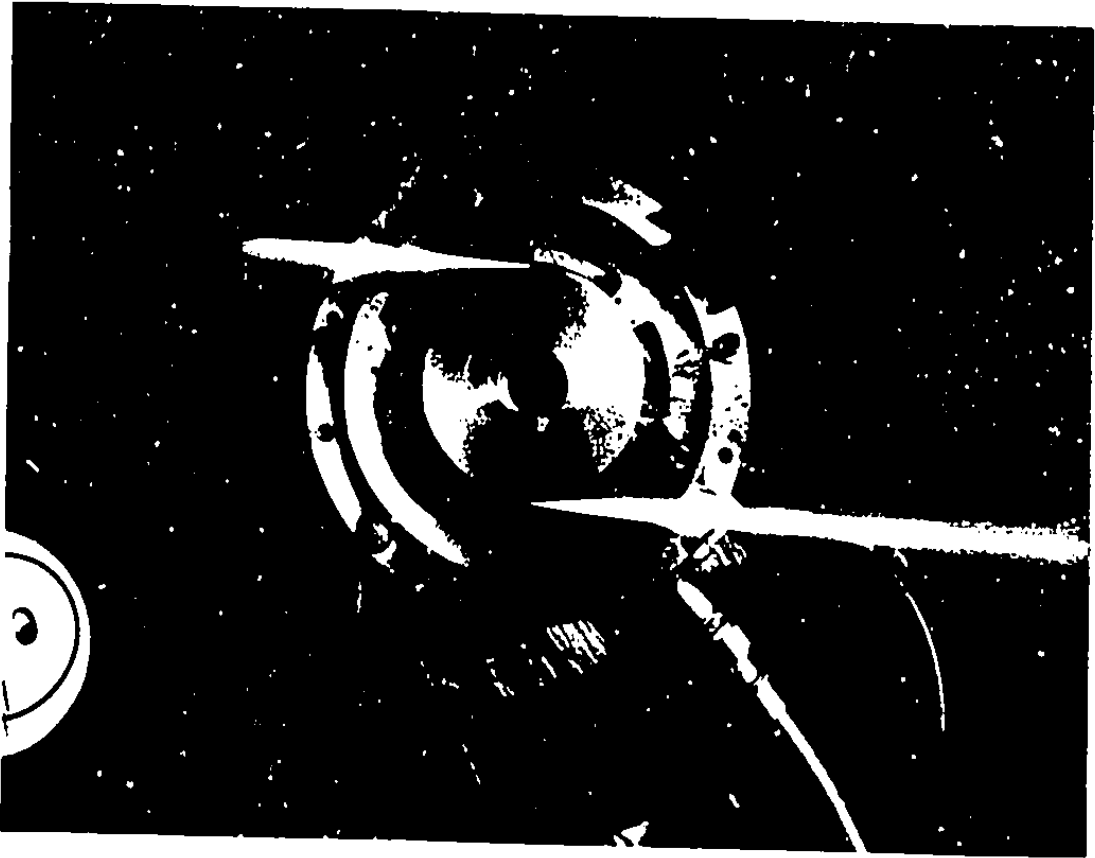


Figure 6. Water Jets from the Two Inlet Nozzles. View
with Rotor and Turbine Housing Removed.

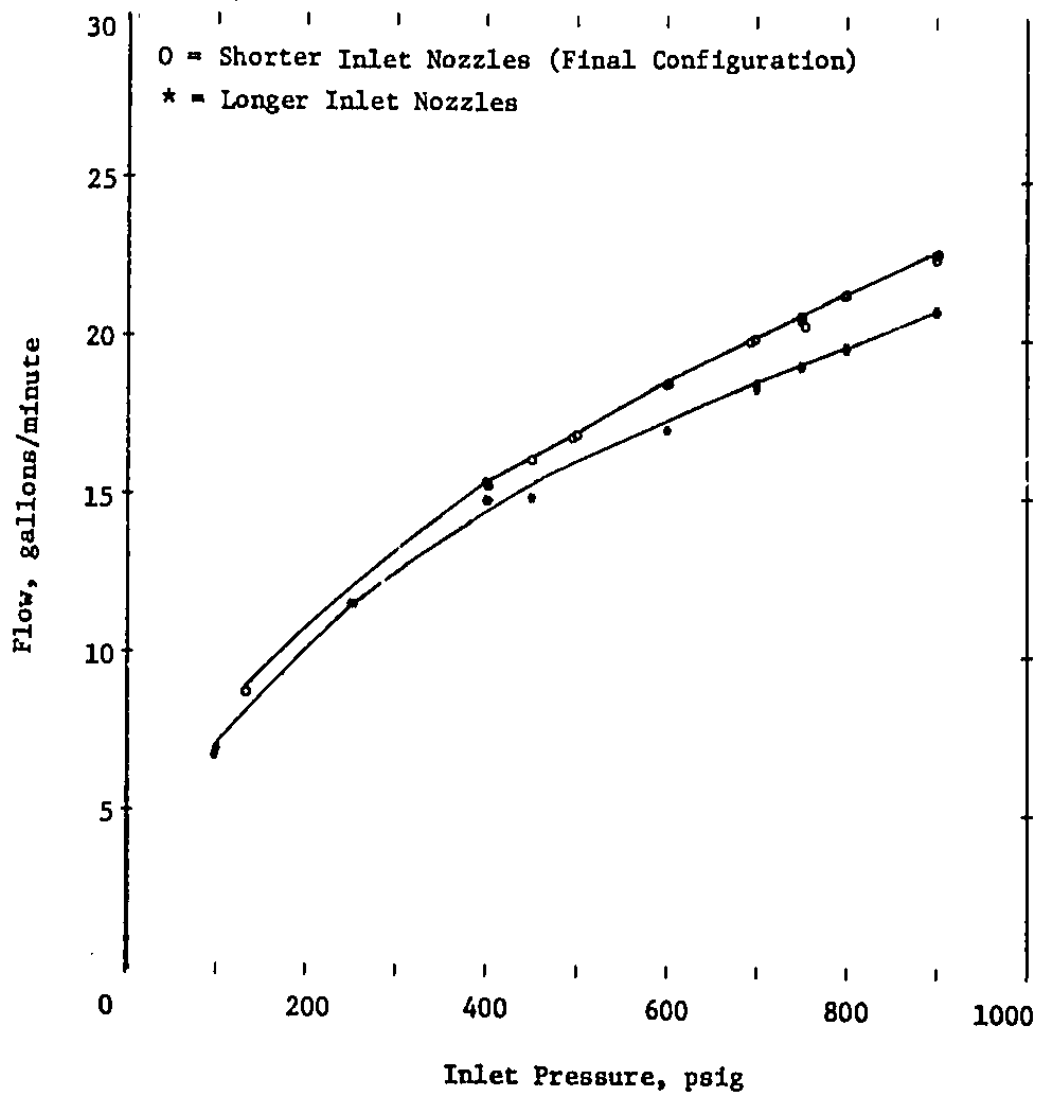


Figure 7. Inlet Nozzle Flow as a Function of Inlet Pressure

Before nozzle-testing, the inlet pressure was increased to 1000 psig in order to verify the pressure capability of the inlet nozzles and inlet manifold. The inlet-manifold and nozzles successfully withstood the 1000-psig inlet pressure.

OVERSPEED TEST

The turbine rotor was spun to 11640 rpm inside the turbine housing. A 1.5 hp motor with variable-speed control replaced the induction generator on the side of the turbine housing for the spin test. The motor was attached to the turbine shaft by a belt. No water flowed through the turbine and the inside of the turbine housing was dry. We spun the rotor to 8,000, 9,000, 10,000, 11,000 and 11,640 rpm. After each run we disassembled the rotor and checked three critical measurements on the rotor for permanent deformation. We observed no changes after any run. 11,640 rpm was the maximum speed possible with the motor and pulley combinations that were available. Based on extrapolation of the variable-speed test data, the run-away speed (no-load speed) for the turbine is 9500 rpm at 500 psig inlet pressure, 11,400 rpm at 750 psig and 12,400 rpm at 900 psig. So the turbine has been tested to runaway speed at 750 psig, which is design-point operation.

VARIABLE-SPEED PERFORMANCE TESTS

We measured turbine performance as a function of rotor speed using the variable-speed hydraulic-pump load system. Torque and speed measurements were made at a constant inlet pressure. The inlet pressure was set by the high-pressure water-supply pump and bypass valve. Then, by varying the load on the turbine with the hydraulic pump, we established steady operation at different speeds. At each speed we checked the inlet pressure and flow, and measured the turbine net-output torque and speed. Appendix A has a tabulation of the test data.

Figure 8 shows the turbine torque as a function of speed. Figure 9 shows the same data plotted as turbine-efficiency as a function of speed. These two figures show data with a constant 750-psig inlet pressure. The figures compare analytical predictions with data from the tests with both the longer inlet nozzles the shorter nozzles.

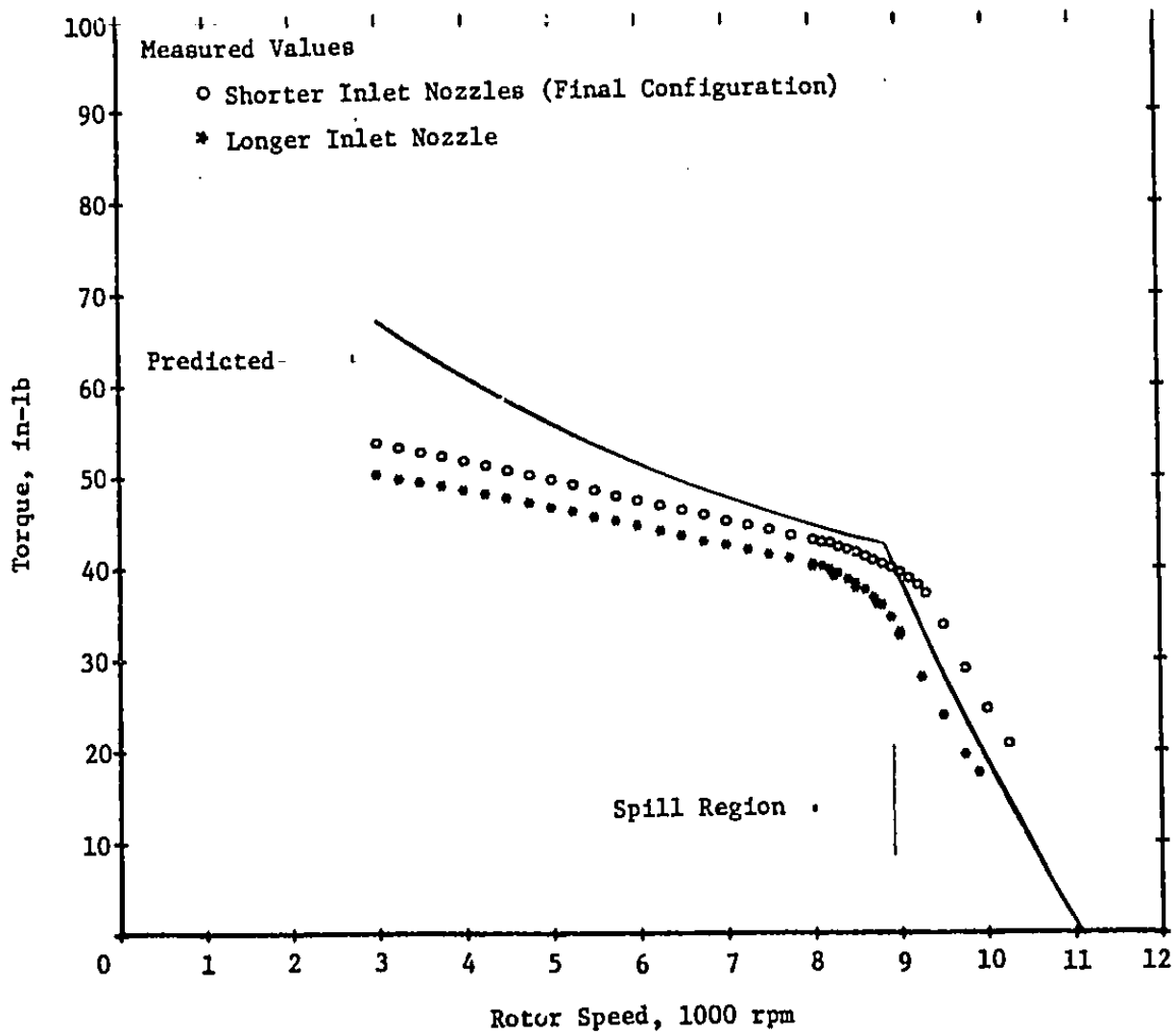


Figure 8. Turbine Net Torque as a Function of Speed at 750-psig Inlet Pressure

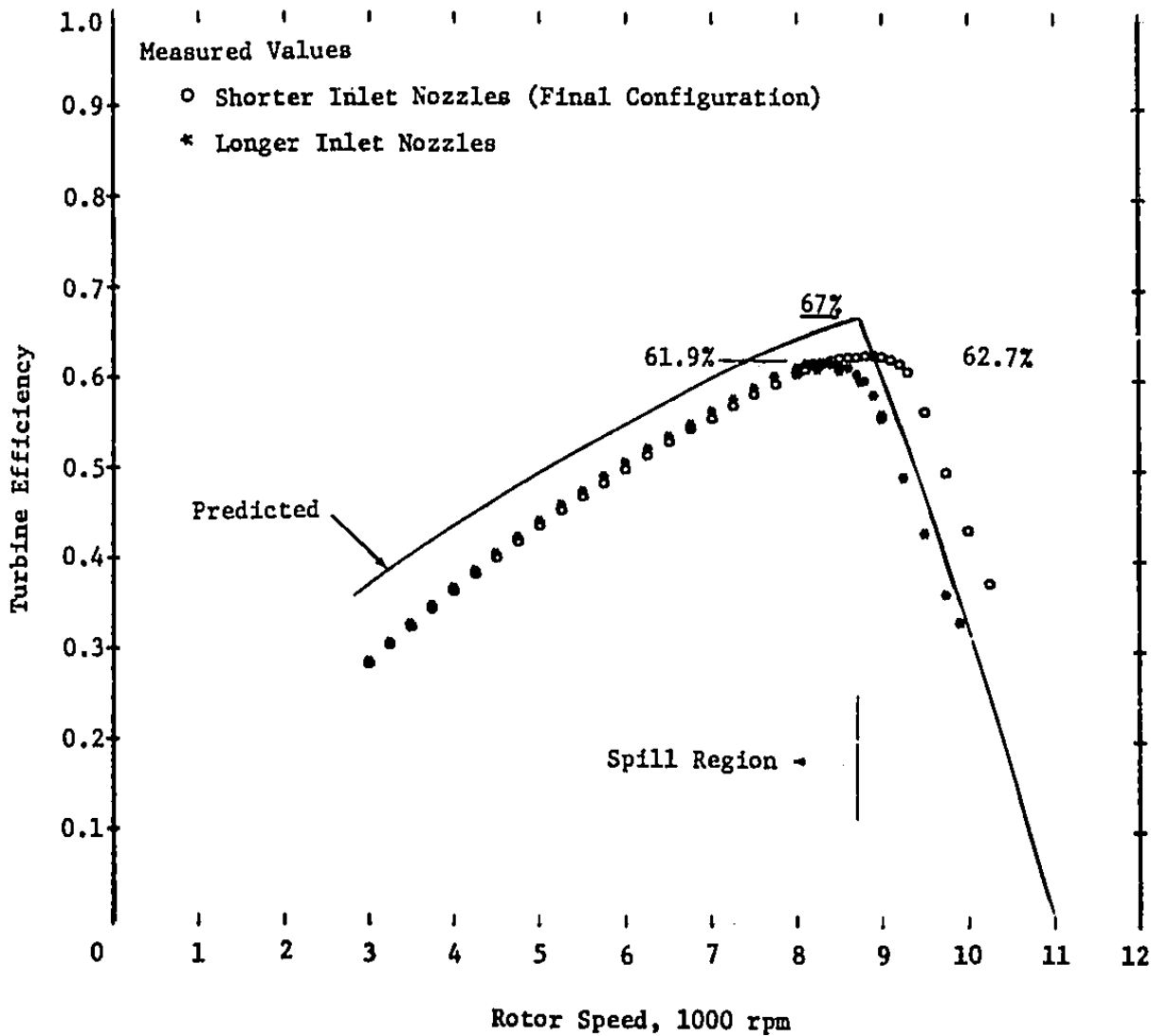


Figure 9. Turbine Efficiency as a Function of Speed at 750 psig Inlet Pressure

Turbine efficiency η_T is calculated by:

$$\eta_T = \frac{\text{net shaft power}}{\text{ideal fluid power}} = \frac{NTC_2}{(P_1 - P_2) Q}$$

where

N = turbine speed, rpm

T = net shaft torque, in-lb

P_1, P_2 = inlet, outlet pressure, psi

Q = volume flowrate, gpm

C_2 = units conversion = .0272

Best efficiency operation occurs at the "knee" in the torque and efficiency curves. With a constant inlet pressure, the flow through the inlet nozzles is fixed. However, the flow capacity of the rotor increases with speed. Higher speeds provide higher centrifugal head to drive more flow out of the rotor jets. At the best-efficiency speed, rotor-flow capacity matches the inlet-nozzle flow capacity.

At speeds lower than the best-efficiency speed, some of the inlet flow spills, by design, from the rotor's inner rim and does not flow through the rotor. The flow moves around the top of the rotor and is directed by the housing into the sump. In this spill region the shorter-inlet nozzle torque is about 8% higher than for the longer inlet nozzles. The higher torque is due to a 7% increase in flow through the shorter nozzles. The efficiency in the spill region is essentially the same for both nozzles.

At the lowest speeds in the spill region, the difference between predicted and measured torque was greatest. The predicted torque was higher due to the assumption that the spilled flow leaves the rotor at the velocity of the inner rim. The flow moves onto this rim from the inlet nozzles at a higher velocity. Actually, the spilled flow does not all slow down to the rim speed before spilling

and so does not impart as much momentum to the rotor as expected. The inlet-nozzle exit velocity is independent of rotor speed at fixed inlet pressure.

At rotor speeds higher than the best-efficiency speed, the rotor is able to pass more flow than the inlet nozzles provide. The rotor passages do not fill completely. The relative velocity of the flow leaving the rotor jets remains the same because inlet flow is the same. If the passages were full, the higher speed rotor would generate a higher relative velocity. So the rotor does not absorb the flow's momentum as effectively. And, torque and efficiency drop as rotor speed increases. Above the best-efficiency speed, predicted torque and efficiency is above the actual data for the longer inlet nozzles because predicted flow (20 gpm) was above actual flow (19.2 gpm). Similarly, the shorter-inlet-nozzle torque and efficiency is higher than predicted due to higher flow (20.6 gpm). Higher flow shifts torque and efficiency curves to the right to higher speed where the rotor flow matches the inlet-nozzle flow.

The inlet nozzle housing contains three viewports. Through the viewports we could observe the flow from the inlet nozzles onto the inner rim of the rotor. During operation near the design speed, the flow was cleaner with the longer inlet nozzles than with the shorter nozzles. The water jets from the nozzles travel about one inch from the nozzle exit to the rotor through the air which surrounds the rotor. The jets from the shorter nozzles diverge more, and the rotor does not capture them as completely. The result is some splash of water droplets between the rotor and housing. The splashed droplets reduce the turbine efficiency because the rotor must reaccelerate these droplets. Despite the increased splash, the turbine efficiency with the shorter nozzles was 1% higher at 62.7%. Higher inlet nozzle efficiency overcame the effect of the splash. Efficiencies near the predicted 67% appear obtainable by adjusting the inlet nozzle shape and the rotor inner-rim shape. The adjustment would provide maximum inlet-nozzle efficiency with minimum splash.

Figures 10 and 11 show the measured turbine net torque and efficiency at different inlet pressures for tests using the shorter inlet nozzles. At the 750-psig design inlet pressure, the best efficiency was 62.7% at 8850 rpm compared with predictions of 67% at 8760 rpm. At the 500 psig secondary design point, best

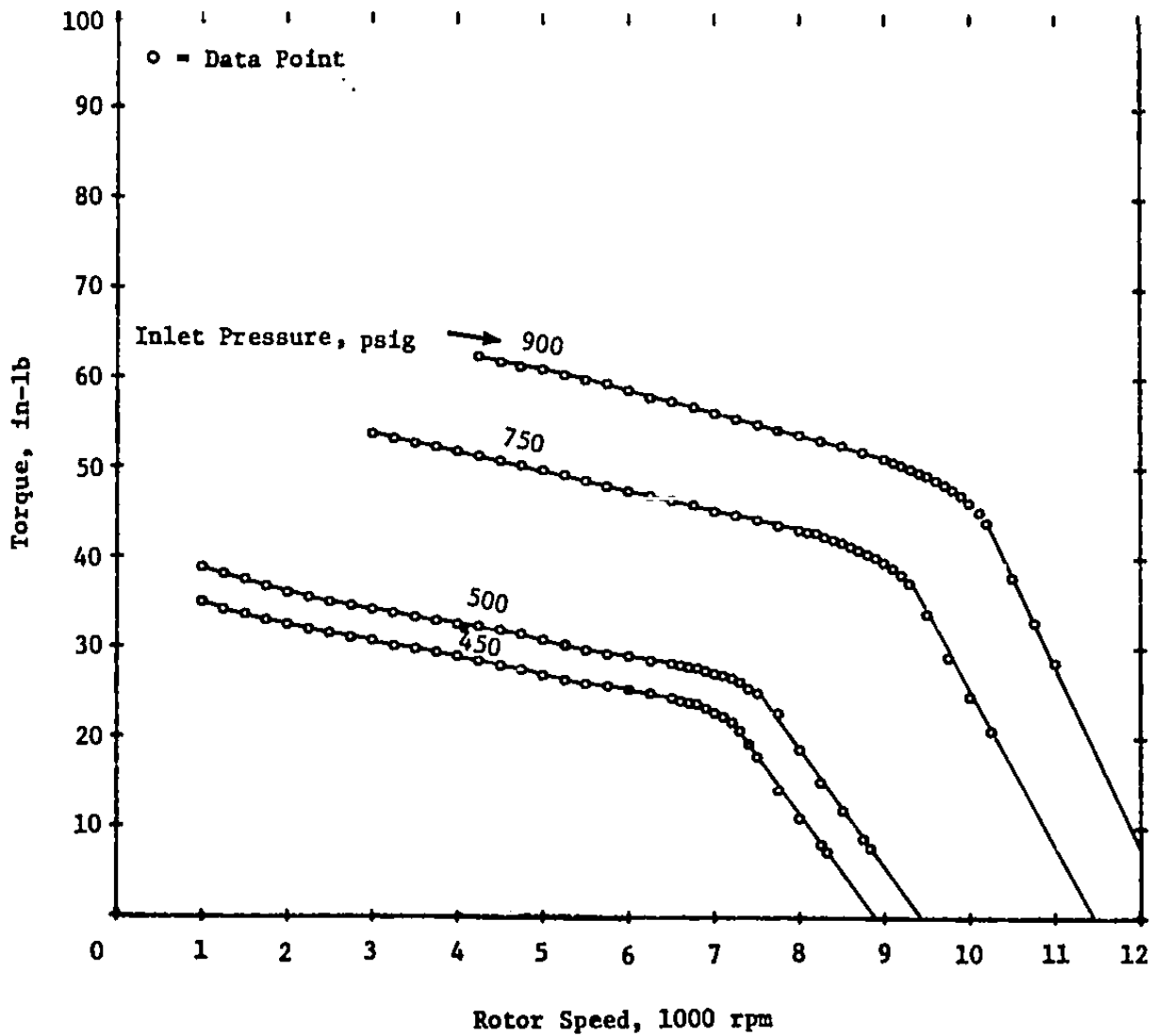


Figure 10. Turbine Net Torque as a Function of Speed

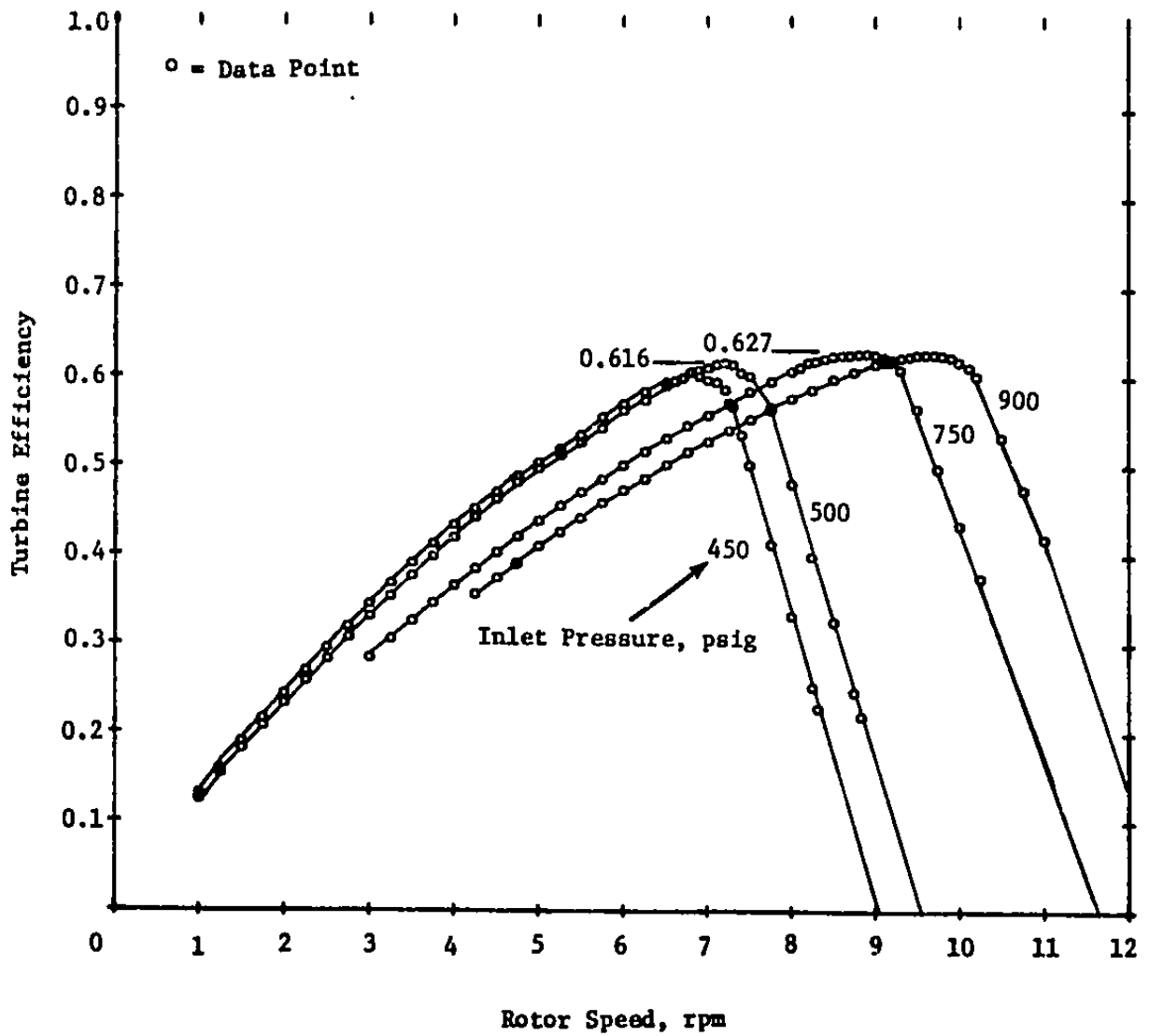


Figure 11. Turbine Efficiency as a Function of Speed

efficiency was 61.6% at 7200 rpm compared with prediction of 66% at 7260 rpm. The uncertainty interval for the efficiency measurement is ± 2 percentage points.

In summary, the efficiency shortfall (62.7% compared to 67% prediction) was mainly due to two factors. First, inlet nozzle efficiency was less than expected. Second, water droplet splash at the rotor inlet slowed the rotor. Both can be corrected by adjustment of the inlet-nozzle shape and rotor-inner-rim shape.

TESTS WITH INDUCTION GENERATOR

Using the turbine to drive a constant-speed generator provides electrical power for possible recycling in the reverse osmosis process. We coupled the turbine to the generator with 2.5- and 6.0-inch pulleys, giving a 2.4 to 1 speed ratio. When no water is flowing to the turbine, and the generator is connected to the power line as a motor, the generator drove the turbine at 8532 rpm. When running at this speed, the turbine and generator began to produce power when the inlet pressure exceeded 475 psig. With 750 psig inlet pressure, the turbine ran at 8650 rpm, producing 4.2 kw of shaft power. Approximate electrical power generated was 3.3 kw giving a generator efficiency of about 79%. Nominal generator efficiency should be 89% and can probably be achieved with power factor adjustment and more precise electrical-power measurement.

Power can be produced at lower inlet pressures more efficiently by switching the turbine drive pulley so that the turbine operates at a lower speed. With a 3-inch pulley, the turbine should run at 7260 rpm and begin generating power when the inlet pressure is above 325 psig, with best efficiency at 500 psig inlet pressure.

PARASITIC LOSSES

We measured windage, bearing and seal losses in a spin-down test. First, with no load, high-pressure water flow accelerated the turbine to 10,000 rpm. Then, we stopped the water flow abruptly and manually recorded

turbine speed every 5 seconds. Separately, we measured the rotating assembly inertia to be 214.51 lbm-in². From the inertia and the speed decay the parasitic losses can be calculated. Figure 12 shows the losses as a function of turbine speed. At 8800 rpm, the measured losses agree with predictions of .44 hp.

VIBRATION

During the turbine testing, we monitored machinery vibration. Velocity-vibration transducers measured axial and radial vibrations on the turbine inlet housing. Figure 13 shows vibration-velocity amplitude as a function of frequency. The turbine was driving the induction generator with 750-psig inlet pressure. The two peaks correspond to the motor speed and the turbine rotor speed. The peaks, at .04 in/sec, are in a range considered acceptable for rotating machinery.

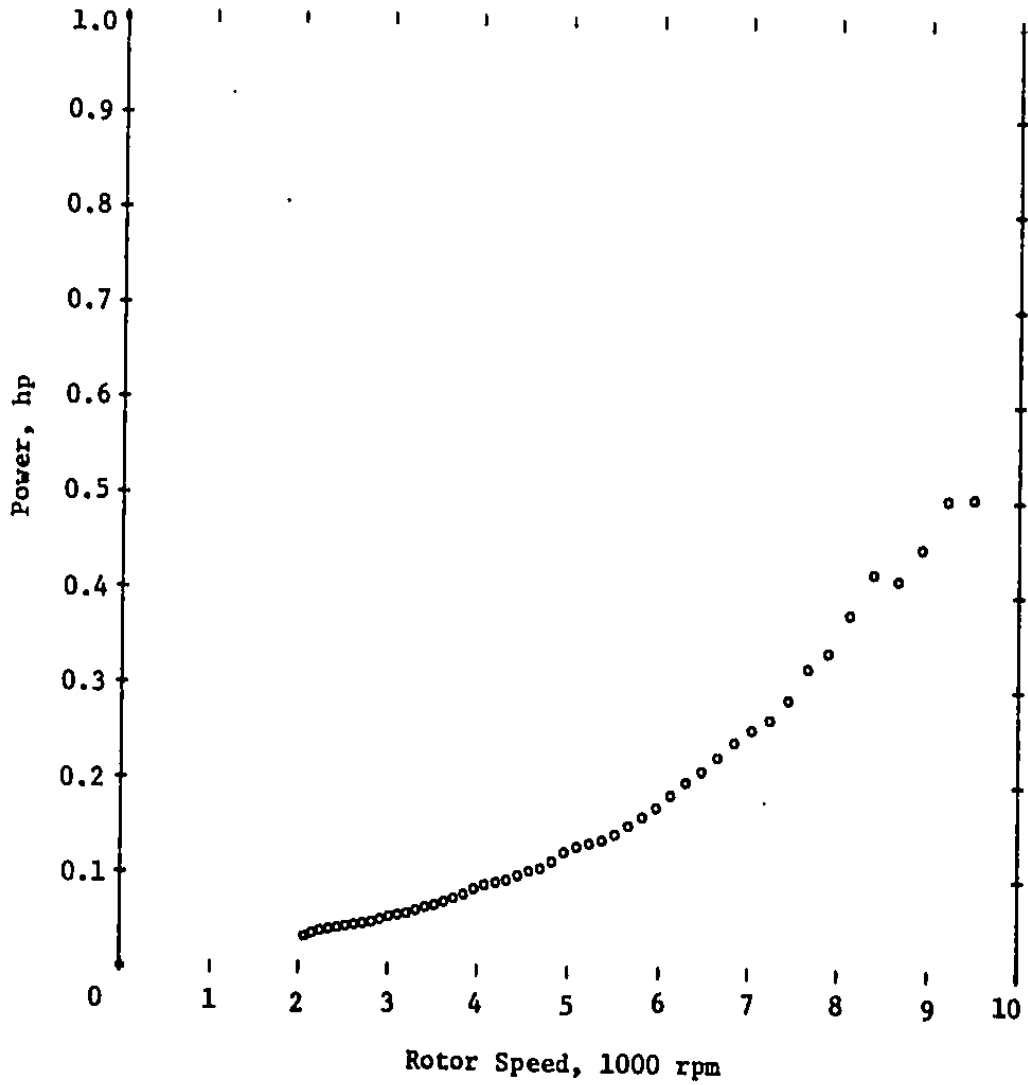


Figure 12. Bearing, Seal and Windage Power (Dry Housing)

Reproduced from
best available copy. 

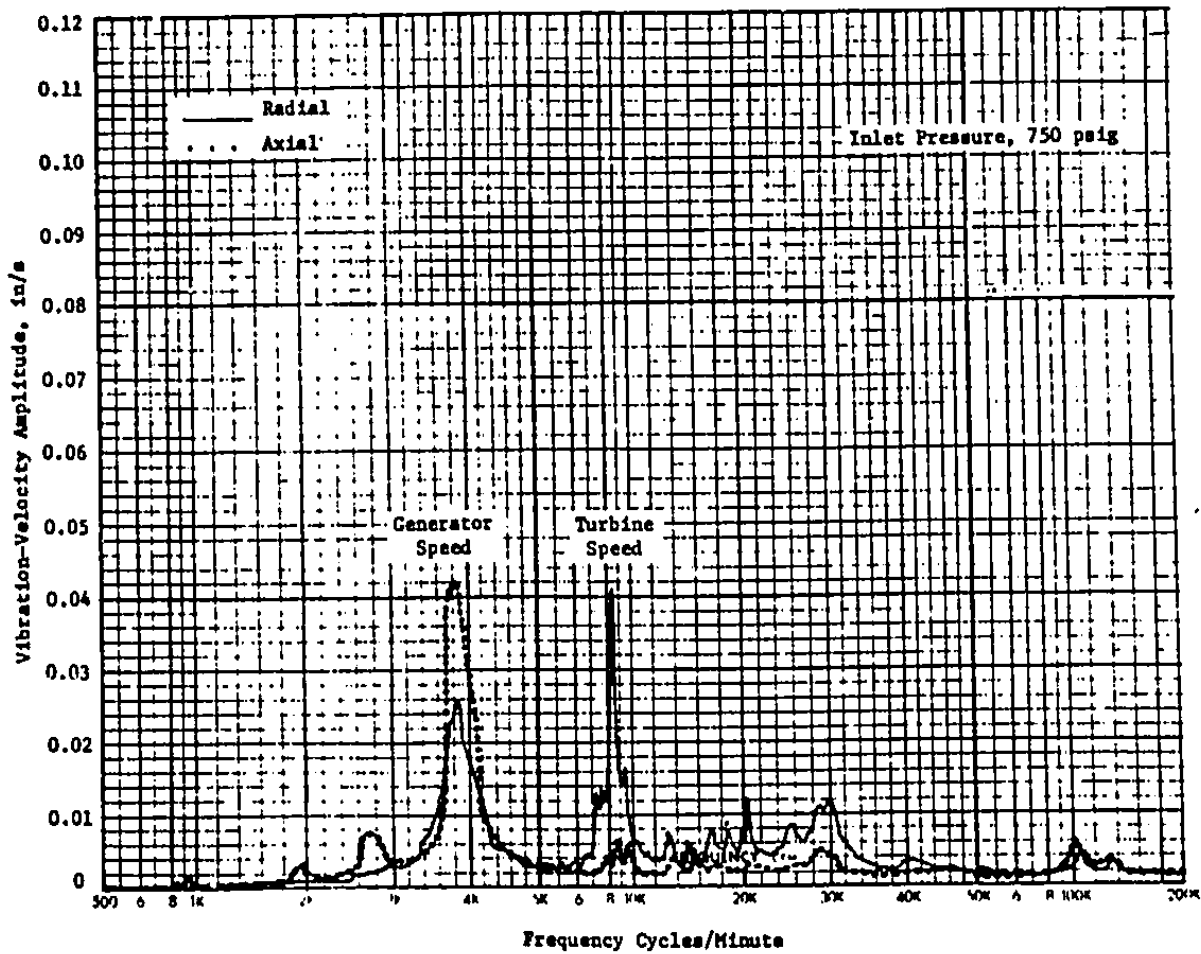


Figure 13. Turbine and Generator Vibration Signature

6. POWER RECOVERY TURBINE FOR LARGER SYSTEMS

The hydraulic reaction turbine can easily handle larger flows. The turbine we have built, with a 10-inch rotor, can handle up to 200-gpm of waste-brine flow with adjustment of the size and number of inlet nozzles and reaction jets. Also, the turbine operating speed can be matched to a specific load by adjusting the rotor size. The best operating speed depends on the inlet pressure and rotor diameter.

We considered design of a turbine for a plant producing 3000 gph of clean water. The power-recovery turbine will have available 100 gpm at 750 psig (for sea-water feed flow). This flow is five times larger than the turbine we have built. We made the following assumptions:

1. A 3000-gph plant requires a 150-gpm high-pressure pump. We assume this pump is a positive-displacement pump such as a Wheatley quintuplex.
2. The turbine feeds recovered power directly to the high-pressure pump (instead of converting power into electricity). This arrangement eliminates the losses associated with an electric generator, which becomes significant at larger turbine-power levels.
3. The design speed was chosen to be 3600 rpm. The resulting turbine diameter is 16.5-inches. (The 600 gph system turbine had a 10-inch diameter.) The turbine can be built with a double-ended horizontal shaft which allows the turbine to be directly coupled to the motor which drives the high-pressure pump. Figure 14 shows the simplified arrangement. The turbine shaft transmits the motor power to the pump. Only one gear reducer is necessary between the turbine and pump.
4. The turbine operates at a single speed, 3600 rpm. This eliminates the requirement to vary the turbine speed as a function of inlet pressure. The system is simpler, at the expense of about 4% on turbine design-point efficiency compared to a variable-speed system.

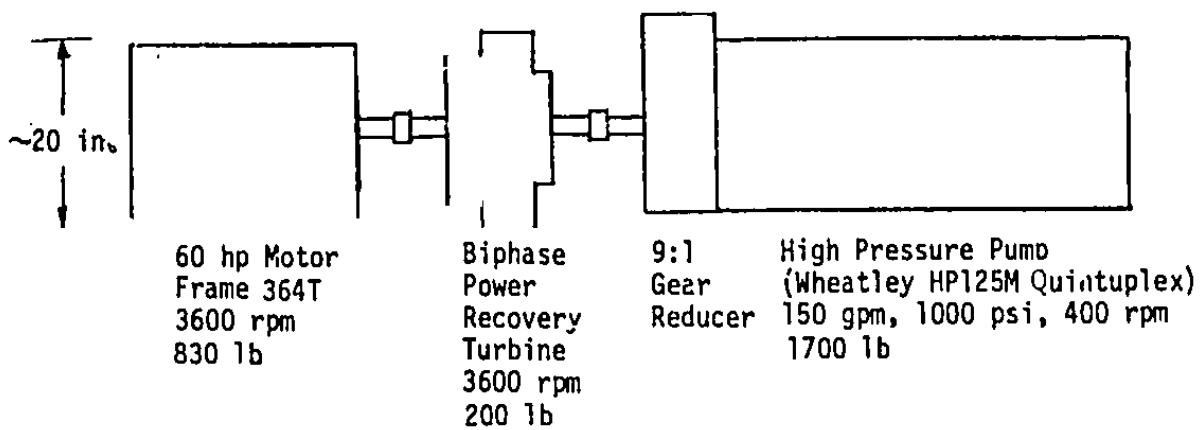


Figure 14. Simplified Mechanical System for 3000 gph RO Desalination System

Figure 15 shows the calculated shaft power recovered by the turbine as a function of inlet pressure. At 500 psig, the turbine recovers 12.4 kW at 70% efficiency. At 750 psig, the turbine recovers 21.6 kW at 66% efficiency. At 750 psig (pump outlet is 800 psig), the pump requires 59.3 kW. The motor requirement is therefore reduced to 37.7 kW of shaft power or 40.6 kW of electrical power (with 93% motor). The efficiency and power predictions are based on the existing turbine design, but with new size, speed and flowrate.

Larger capacity is possible. The 16.5-inch diameter turbine can handle up to 500 gpm and produce 100 kW. Also the turbine can be coupled to a centrifugal pump, verticle-turbine pump or a KOBE pitot-type pump. These pumps run at a higher speed than the positive displacement pumps so that the gear reducer between the turbine and pump can be eliminated. And these pumps can be lighter weight and operate smoother than positive displacement pumps. However, pump efficiency is usually lower.

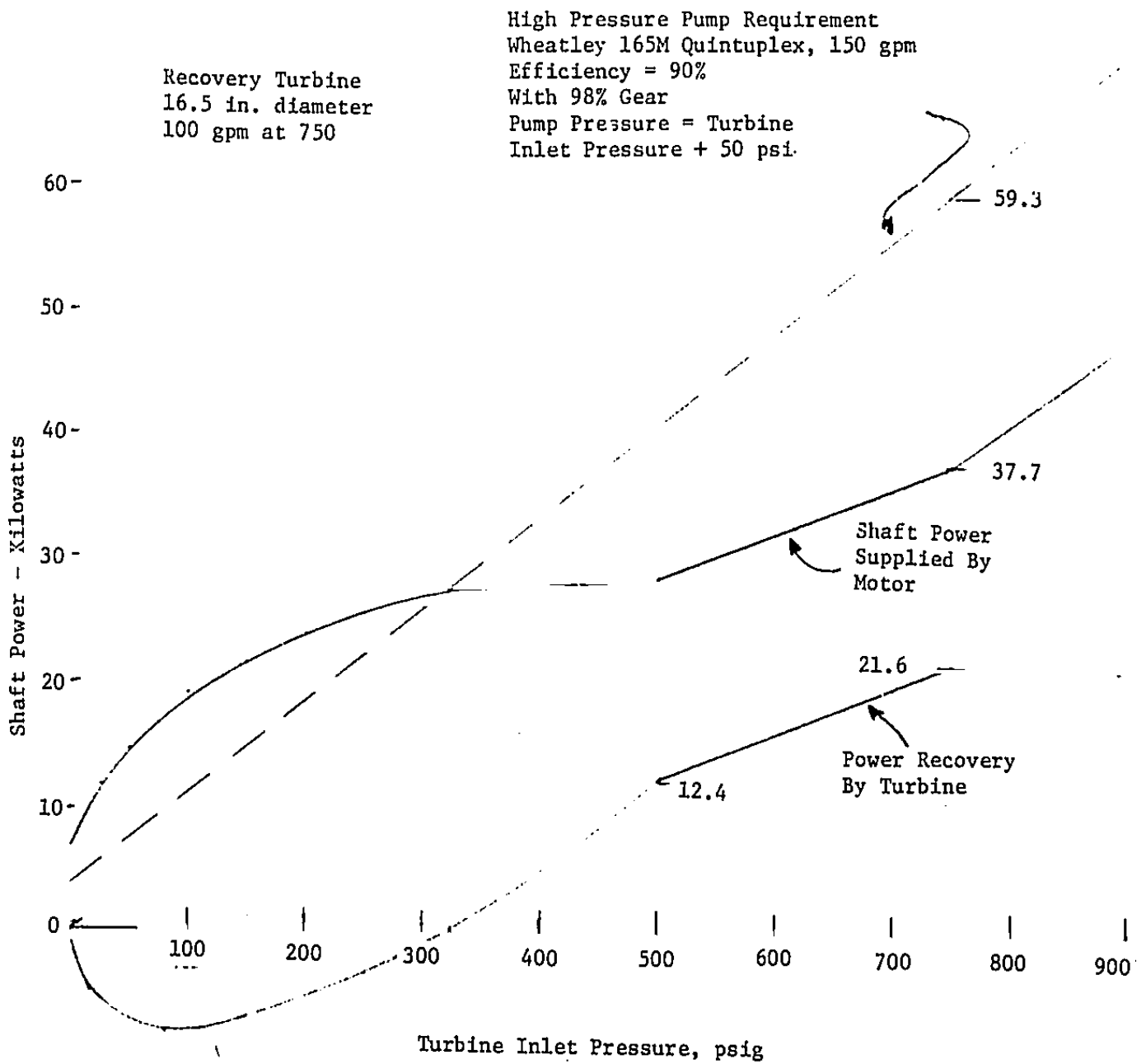


Figure 15. Recovered Power for Turbine for 3000 gph System

7. INCREASED POWER BY WASTE-BRINE HEATING

The power produced by the power-recovery turbine can be increased by heating the waste-brine stream before the brine flows through the turbine. The flow through the turbine becomes a two-phase mixture of brine and steam. However, the heat required for a practicable turbine-power increase is large. The heat requirement is too large to be supplied by the waste heat from the diesel engine which would power the reverse-osmosis plant.

Figure 16 shows the configuration in which the waste brine is heated by engine-exhaust-gas waste heat. For a system which produces 3000 gph of product water from seawater, the waste brine stream from the RO modules is 100 gpm at 750 psig. The power-recovery turbine drives the high-pressure pump which requires 60 kW shaft power. A motor supplies the additional pump power.

When the waste-brine stream is unheated the power-recovery turbine will produce 22.9 kW shaft power (70% efficiency). Figure 17 shows how the turbine power output increases when the waste brine is heated. At a turbine inlet temperature of 245°F, the turbine generates 30.8 kW. The heat required to raise the brine from 210°F to 245°F is 475 Btu/sec or 500 kW. A diesel engine driving a 60 kW electric generator will produce no more than 120 kW of waste heat in the exhaust gas and cooling water. So sufficient waste heat is not available to provide an economical increase in turbine power.

Reducing the turbine outlet pressure below 0 psig will reduce the heat input required. However, a more complicated subatmospheric condensing system would be needed.

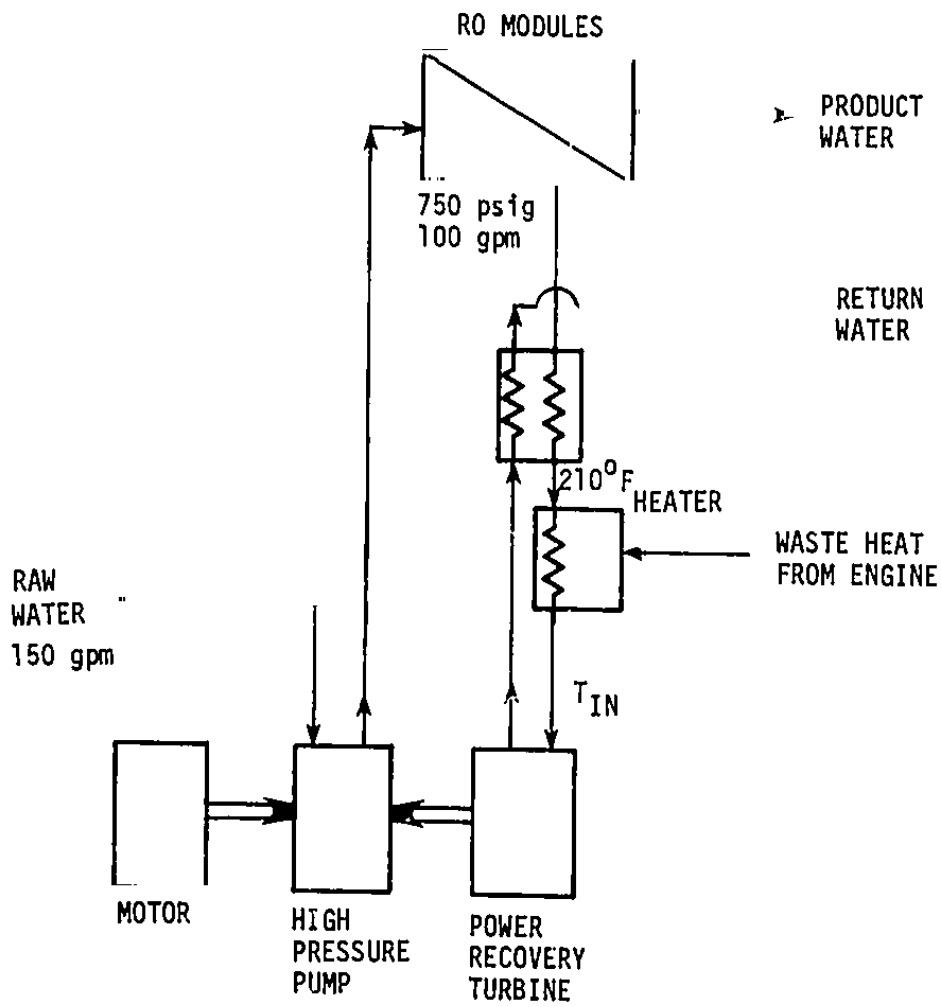
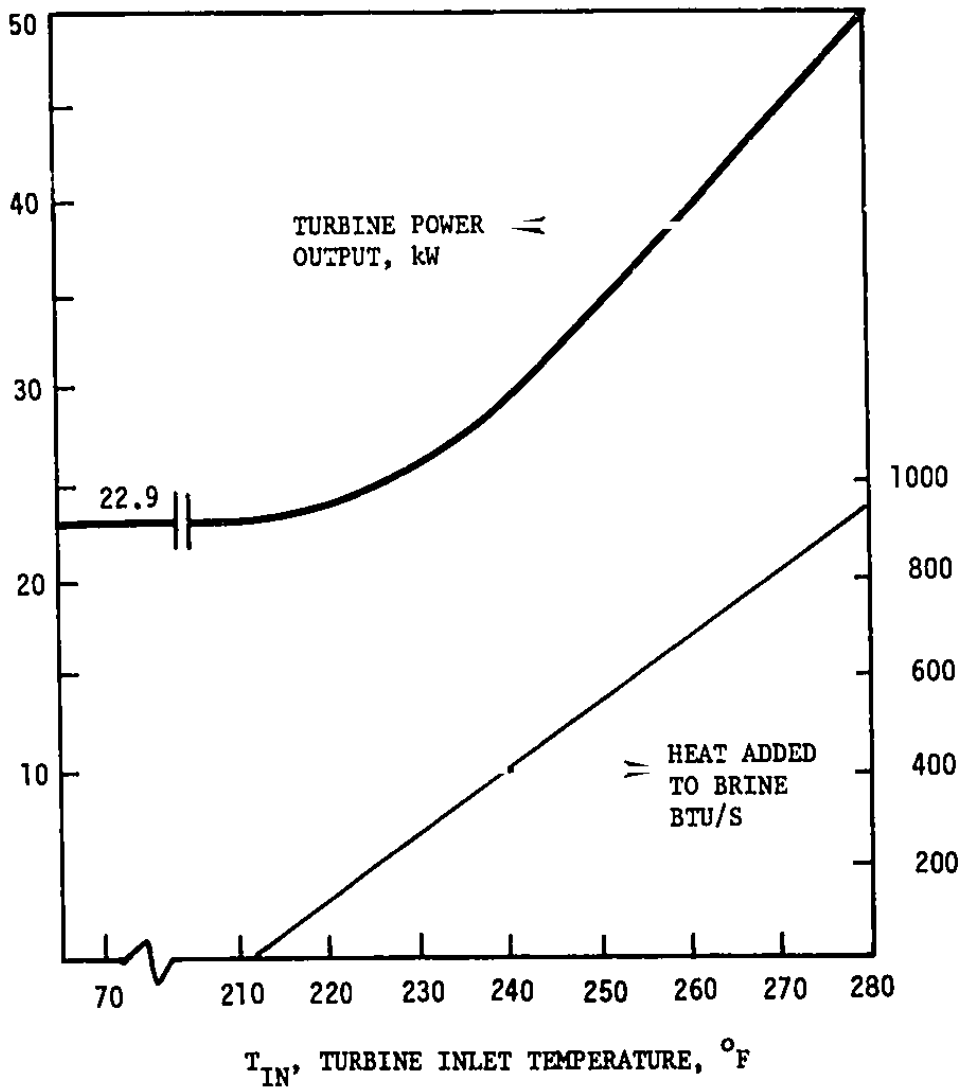


Figure 16. Power Recovery System with Heat Addition



Flow: 20 gpm = 14.3 lbm/s
 Inlet pressure: 750 psig
 Outlet pressure: 0 psig
 Single phase flow to inlet nozzles, two-phase
 flow in rotor

Figure 17. Turbine Power with Heated Brine

8. RECOMMENDATIONS

Performance tests of the new power-recovery reaction turbine are complete. Tests should now begin which would verify the longer term reliability and maintainability of the turbine in reverse osmosis plant service. The tests should be conducted using seawater (or concentrated seawater) in the turbine. (Performance tests were run with fresh water).

We recommend the following:

1. Conduct a 2000-hour reliability test of the power-recover turbine in a seawater flow-loop or connected to a 600 gph Reverse Osmosis Water Purification Unit.
2. Prepare design of a combined package of a high-pressure pump and the reaction power-recovery turbine for larger RO systems.
3. Perform comparison of cost, weight, reliability and performance of the reaction turbine with alternate methods of power recovery.

APPENDIX A

Turbine Performance Data

Data with Longer Inlet Nozzles

<u>Measurements</u>				<u>Calculated Results</u>			
Inlet Temp.	Inlet Pres.	ΔP	Torque	Flow	Torque	Net Power	Efficiency
°F	psia	in.H ₂ O	RPM	gpm	in lb	Hp	
73.4	450	14.5	5000	14.9	25.63	2.03	0.519
73.4	450	14.5	6002	14.9	23.85	2.27	0.580
73.4	450	14.5	7000	14.9	19.38	2.15	0.549
73.4	450	14.5	8000	14.9	6.88	0.87	0.223
73.4	450	14.5	7753	14.9	9.43	1.17	0.298
73.4	450	14.5	7500	14.9	12.50	1.49	0.380
73.4	450	14.5	7250	14.9	15.73	1.81	0.462
73.4	450	14.5	7001	14.9	19.06	2.12	0.540
73.4	450	14.5	6755	14.9	21.25	2.28	0.581
73.4	450	14.5	6499	14.9	22.50	2.32	0.587
73.4	450	14.5	6267	14.9	23.23	2.31	0.583
73.4	450	14.5	6003	14.9	23.65	2.25	0.575
73.4	450	14.5	5754	14.9	24.17	2.21	0.567
73.4	450	14.5	5529	14.9	24.48	2.14	0.548
73.4	450	14.5	5257	14.9	25.00	2.05	0.525
73.4	450	14.5	5004	14.9	25.71	2.01	0.513
73.4	450	14.5	4760	14.9	26.32	1.95	0.500
73.4	450	14.5	4530	14.9	26.85	1.89	0.488
73.4	450	14.5	4300	14.9	27.36	1.83	0.476
73.4	450	14.5	4080	14.9	27.85	1.77	0.464
73.4	450	14.5	3870	14.9	28.32	1.71	0.452
73.4	450	14.5	3670	14.9	28.77	1.65	0.440
73.4	450	14.5	3480	14.9	29.20	1.59	0.428
73.4	450	14.5	3300	14.9	29.61	1.53	0.416
73.4	450	14.5	3130	14.9	30.00	1.47	0.404
73.4	450	14.5	2970	14.9	30.36	1.41	0.392
73.4	450	14.5	2820	14.9	30.70	1.35	0.380
73.4	450	14.5	2680	14.9	31.01	1.29	0.368
73.4	450	14.5	2550	14.9	31.29	1.23	0.356
73.4	450	14.5	2430	14.9	31.55	1.17	0.344
73.4	450	14.5	2320	14.9	31.78	1.11	0.332
73.4	450	14.5	2220	14.9	32.00	1.05	0.320
73.4	450	14.5	2130	14.9	32.19	1.00	0.308
73.4	450	14.5	2050	14.9	32.35	0.95	0.296
73.4	450	14.5	1980	14.9	32.48	0.90	0.284
73.4	450	14.5	1920	14.9	32.58	0.86	0.272
73.4	450	14.5	1870	14.9	32.65	0.82	0.260
73.4	450	14.5	1830	14.9	32.70	0.78	0.248
73.4	450	14.5	1800	14.9	32.73	0.75	0.236
73.4	450	14.5	1780	14.9	32.74	0.72	0.224
73.4	450	14.5	1770	14.9	32.74	0.70	0.212
73.4	450	14.5	1770	14.9	32.73	0.68	0.200
73.4	450	14.5	1770	14.9	32.70	0.66	0.188
73.4	450	14.5	1770	14.9	32.65	0.64	0.176
73.4	450	14.5	1770	14.9	32.58	0.62	0.164
73.4	450	14.5	1770	14.9	32.48	0.60	0.152
73.4	450	14.5	1770	14.9	32.35	0.58	0.140
73.4	450	14.5	1770	14.9	32.19	0.56	0.128
73.4	450	14.5	1770	14.9	32.00	0.54	0.116
73.4	450	14.5	1770	14.9	31.78	0.52	0.104
73.4	450	14.5	1770	14.9	31.55	0.50	0.092
73.4	450	14.5	1770	14.9	31.29	0.48	0.080
73.4	450	14.5	1770	14.9	31.01	0.46	0.068
73.4	450	14.5	1770	14.9	30.70	0.44	0.056
73.4	450	14.5	1770	14.9	30.36	0.42	0.044
73.4	450	14.5	1770	14.9	30.00	0.40	0.032
73.4	450	14.5	1770	14.9	29.61	0.38	0.020
73.4	450	14.5	1770	14.9	29.19	0.36	0.008
73.4	450	14.5	1770	14.9	28.75	0.34	0.000

Data with Longer Inlet Nozzles

<u>Measurements</u>					<u>Calculated Results</u>			
Inlet Temp. °F	Inlet Pres. psia	Flow ΔP in. H ₂ O	RPM	Torque readout	Flow gpm	Torque in lb	Net Power Hp	Efficiency
72.4	750	23.7	2500	403	19.1	50.31	2.39	0.386
72.4	750	23.7	2557	417	19.1	49.74	2.47	0.397
72.4	750	23.7	2605	425	19.1	49.44	2.74	0.428
72.4	750	23.7	2742	437	19.1	49.36	2.51	0.449
72.4	750	23.7	2900	446	19.1	49.54	2.69	0.479
72.4	750	23.7	3049	452	19.1	49.72	2.74	0.491
72.4	750	23.7	3194	458	19.1	49.71	2.40	0.497
72.4	750	23.7	3250	459	19.1	47.19	2.55	0.495
72.4	750	23.7	3403	448	19.1	46.67	2.79	0.466
72.4	750	23.7	3555	444	19.1	46.25	2.96	0.467
72.4	750	23.7	3662	438	19.1	45.63	2.96	0.476
72.4	750	23.7	3748	434	19.1	45.21	2.77	0.467
72.4	750	23.7	3996	425	19.1	44.69	2.75	0.503
72.4	750	23.7	4158	425	19.1	44.06	2.72	0.522
72.4	750	23.7	4300	418	19.1	43.54	2.49	0.537
72.4	750	23.7	4454	417	19.1	42.92	2.60	0.550
72.4	750	23.7	4605	408	19.1	42.50	2.77	0.565
72.4	750	23.7	4756	401	19.1	41.38	2.83	0.576
72.5	750	23.7	4902	398	19.1	41.46	2.74	0.540
72.5	750	23.7	5044	394	19.1	41.04	2.94	0.603
72.5	750	23.7	5200	385	19.1	40.10	2.89	0.609
72.5	750	23.7	5347	375	19.1	39.66	2.81	0.611
72.5	750	23.7	5500	363	19.1	37.91	2.80	0.610
72.5	750	23.7	5649	346	19.1	36.64	2.80	0.598
72.5	750	23.7	5898	312	19.1	32.60	2.65	0.557
72.5	750	23.7	6250	269	19.1	28.02	2.11	0.492
72.5	750	23.7	6500	229	19.1	25.85	1.60	0.430
72.5	750	23.7	6748	188	19.1	19.58	1.03	0.362
72.5	750	23.7	6906	169	19.1	17.60	0.77	0.331
69.3	750	23.8	8007	388	19.1	40.42	2.83	0.613
69.3	750	23.8	8113	386	19.1	40.21	2.88	0.618
69.3	750	23.8	8200	382	19.1	39.79	2.88	0.618
69.3	750	23.8	8296	378	19.1	39.38	2.88	0.619
69.3	750	23.8	8407	372	19.1	38.75	2.87	0.617
69.3	750	23.8	8504	367	19.1	38.21	2.86	0.616
69.3	750	23.8	8609	361	19.1	37.60	2.84	0.613
69.3	750	23.8	8705	353	19.1	36.77	2.80	0.606
69.3	750	23.8	8800	345	19.1	35.94	2.76	0.599
69.3	750	23.8	8903	332	19.1	34.58	2.69	0.583
69.3	750	23.8	9001	316	19.1	32.92	2.50	0.561

Data with Longer Inlet Nozzles

<u>Measurements</u>					<u>Calculated Results</u>			
Inlet Temp. °F	Inlet Pres. psig	Flow ΔP in. H ₂ O	RPM	Torque readout	Flow gpm	Torque in lb	Net Power Hp	Efficiency
70.0	100	1.0	1000	100	10.0	100	1.0	0.400
70.0	100	2.0	1000	200	20.0	200	2.0	0.400
70.0	100	3.0	1000	300	30.0	300	3.0	0.400
70.0	100	4.0	1000	400	40.0	400	4.0	0.400
70.0	100	5.0	1000	500	50.0	500	5.0	0.400
70.0	100	6.0	1000	600	60.0	600	6.0	0.400
70.0	100	7.0	1000	700	70.0	700	7.0	0.400
70.0	100	8.0	1000	800	80.0	800	8.0	0.400
70.0	100	9.0	1000	900	90.0	900	9.0	0.400
70.0	100	10.0	1000	1000	100.0	1000	10.0	0.400
70.0	100	11.0	1000	1100	110.0	1100	11.0	0.400
70.0	100	12.0	1000	1200	120.0	1200	12.0	0.400
70.0	100	13.0	1000	1300	130.0	1300	13.0	0.400
70.0	100	14.0	1000	1400	140.0	1400	14.0	0.400
70.0	100	15.0	1000	1500	150.0	1500	15.0	0.400
70.0	100	16.0	1000	1600	160.0	1600	16.0	0.400
70.0	100	17.0	1000	1700	170.0	1700	17.0	0.400
70.0	100	18.0	1000	1800	180.0	1800	18.0	0.400
70.0	100	19.0	1000	1900	190.0	1900	19.0	0.400
70.0	100	20.0	1000	2000	200.0	2000	20.0	0.400
70.0	100	21.0	1000	2100	210.0	2100	21.0	0.400
70.0	100	22.0	1000	2200	220.0	2200	22.0	0.400
70.0	100	23.0	1000	2300	230.0	2300	23.0	0.400
70.0	100	24.0	1000	2400	240.0	2400	24.0	0.400
70.0	100	25.0	1000	2500	250.0	2500	25.0	0.400
70.0	100	26.0	1000	2600	260.0	2600	26.0	0.400
70.0	100	27.0	1000	2700	270.0	2700	27.0	0.400
70.0	100	28.0	1000	2800	280.0	2800	28.0	0.400
70.0	100	29.0	1000	2900	290.0	2900	29.0	0.400
70.0	100	30.0	1000	3000	300.0	3000	30.0	0.400
70.0	100	31.0	1000	3100	310.0	3100	31.0	0.400
70.0	100	32.0	1000	3200	320.0	3200	32.0	0.400
70.0	100	33.0	1000	3300	330.0	3300	33.0	0.400
70.0	100	34.0	1000	3400	340.0	3400	34.0	0.400
70.0	100	35.0	1000	3500	350.0	3500	35.0	0.400
70.0	100	36.0	1000	3600	360.0	3600	36.0	0.400
70.0	100	37.0	1000	3700	370.0	3700	37.0	0.400
70.0	100	38.0	1000	3800	380.0	3800	38.0	0.400
70.0	100	39.0	1000	3900	390.0	3900	39.0	0.400
70.0	100	40.0	1000	4000	400.0	4000	40.0	0.400
70.0	100	41.0	1000	4100	410.0	4100	41.0	0.400
70.0	100	42.0	1000	4200	420.0	4200	42.0	0.400
70.0	100	43.0	1000	4300	430.0	4300	43.0	0.400
70.0	100	44.0	1000	4400	440.0	4400	44.0	0.400
70.0	100	45.0	1000	4500	450.0	4500	45.0	0.400
70.0	100	46.0	1000	4600	460.0	4600	46.0	0.400
70.0	100	47.0	1000	4700	470.0	4700	47.0	0.400
70.0	100	48.0	1000	4800	480.0	4800	48.0	0.400
70.0	100	49.0	1000	4900	490.0	4900	49.0	0.400
70.0	100	50.0	1000	5000	500.0	5000	50.0	0.400
70.0	100	51.0	1000	5100	510.0	5100	51.0	0.400
70.0	100	52.0	1000	5200	520.0	5200	52.0	0.400
70.0	100	53.0	1000	5300	530.0	5300	53.0	0.400
70.0	100	54.0	1000	5400	540.0	5400	54.0	0.400
70.0	100	55.0	1000	5500	550.0	5500	55.0	0.400
70.0	100	56.0	1000	5600	560.0	5600	56.0	0.400
70.0	100	57.0	1000	5700	570.0	5700	57.0	0.400
70.0	100	58.0	1000	5800	580.0	5800	58.0	0.400
70.0	100	59.0	1000	5900	590.0	5900	59.0	0.400
70.0	100	60.0	1000	6000	600.0	6000	60.0	0.400
70.0	100	61.0	1000	6100	610.0	6100	61.0	0.400
70.0	100	62.0	1000	6200	620.0	6200	62.0	0.400
70.0	100	63.0	1000	6300	630.0	6300	63.0	0.400
70.0	100	64.0	1000	6400	640.0	6400	64.0	0.400
70.0	100	65.0	1000	6500	650.0	6500	65.0	0.400
70.0	100	66.0	1000	6600	660.0	6600	66.0	0.400
70.0	100	67.0	1000	6700	670.0	6700	67.0	0.400
70.0	100	68.0	1000	6800	680.0	6800	68.0	0.400
70.0	100	69.0	1000	6900	690.0	6900	69.0	0.400
70.0	100	70.0	1000	7000	700.0	7000	70.0	0.400
70.0	100	71.0	1000	7100	710.0	7100	71.0	0.400
70.0	100	72.0	1000	7200	720.0	7200	72.0	0.400
70.0	100	73.0	1000	7300	730.0	7300	73.0	0.400
70.0	100	74.0	1000	7400	740.0	7400	74.0	0.400
70.0	100	75.0	1000	7500	750.0	7500	75.0	0.400
70.0	100	76.0	1000	7600	760.0	7600	76.0	0.400
70.0	100	77.0	1000	7700	770.0	7700	77.0	0.400
70.0	100	78.0	1000	7800	780.0	7800	78.0	0.400
70.0	100	79.0	1000	7900	790.0	7900	79.0	0.400
70.0	100	80.0	1000	8000	800.0	8000	80.0	0.400
70.0	100	81.0	1000	8100	810.0	8100	81.0	0.400
70.0	100	82.0	1000	8200	820.0	8200	82.0	0.400
70.0	100	83.0	1000	8300	830.0	8300	83.0	0.400
70.0	100	84.0	1000	8400	840.0	8400	84.0	0.400
70.0	100	85.0	1000	8500	850.0	8500	85.0	0.400
70.0	100	86.0	1000	8600	860.0	8600	86.0	0.400
70.0	100	87.0	1000	8700	870.0	8700	87.0	0.400
70.0	100	88.0	1000	8800	880.0	8800	88.0	0.400
70.0	100	89.0	1000	8900	890.0	8900	89.0	0.400
70.0	100	90.0	1000	9000	900.0	9000	90.0	0.400
70.0	100	91.0	1000	9100	910.0	9100	91.0	0.400
70.0	100	92.0	1000	9200	920.0	9200	92.0	0.400
70.0	100	93.0	1000	9300	930.0	9300	93.0	0.400
70.0	100	94.0	1000	9400	940.0	9400	94.0	0.400
70.0	100	95.0	1000	9500	950.0	9500	95.0	0.400
70.0	100	96.0	1000	9600	960.0	9600	96.0	0.400
70.0	100	97.0	1000	9700	970.0	9700	97.0	0.400
70.0	100	98.0	1000	9800	980.0	9800	98.0	0.400
70.0	100	99.0	1000	9900	990.0	9900	99.0	0.400
70.0	100	100.0	1000	10000	1000.0	10000	100.0	0.400

Data with Shorter Inlet Nozzles (final configuration)

Measurements					Calculated Results			
Inlet Temp. °F	Inlet Pres. psia	Flow ΔP in. H ₂ O	RPM	Torque readout	Flow gpm	Torque in lb	Net Power Hp	Efficiency
69.1	450	17.0	1000	336	16.2	35.00	0.56	0.131
69.1	450	17.0	1247	320	16.2	34.17	0.52	0.159
69.1	450	16.9	1503	323	16.1	33.65	0.80	0.190
69.3	450	17.0	1747	317	16.2	33.02	0.92	0.216
69.3	450	17.0	2000	312	16.2	32.50	1.03	0.243
69.3	450	17.0	2250	307	16.2	31.92	1.14	0.269
69.4	450	17.0	2497	303	16.2	31.56	1.25	0.295
69.4	450	17.0	2746	298	16.2	31.04	1.35	0.319
69.4	450	17.0	2998	295	16.2	30.73	1.46	0.344
69.4	450	16.9	3257	289	16.1	30.10	1.56	0.368
70.7	450	17.0	3507	286	16.2	29.79	1.66	0.391
70.7	450	17.0	3755	282	16.2	29.38	1.75	0.412
70.7	450	17.0	4002	276	16.2	28.96	1.84	0.433
70.6	450	17.0	4247	273	16.2	28.44	1.92	0.451
70.7	450	17.0	4506	268	16.2	27.92	2.00	0.470
70.7	450	17.0	4754	264	16.2	27.50	2.07	0.489
70.7	450	16.9	5000	258	16.1	26.88	2.13	0.504
70.7	450	16.9	5253	253	16.1	26.35	2.20	0.519
70.7	450	16.9	5499	249	16.1	25.94	2.26	0.535
70.7	450	16.9	5752	247	16.1	25.73	2.35	0.555
70.7	450	16.9	6003	243	16.1	25.31	2.41	0.570
70.7	450	16.9	6252	239	16.1	24.90	2.47	0.583
70.7	450	16.9	6502	234	16.1	24.38	2.51	0.594
71.2	450	16.9	6602	231	16.1	24.06	2.52	0.596
71.2	450	16.9	6703	229	16.1	23.85	2.54	0.599
71.2	450	16.9	6795	228	16.1	23.75	2.56	0.605
71.2	450	16.9	6900	223	16.1	23.23	2.54	0.601
71.2	450	16.9	7001	218	16.1	22.71	2.52	0.596
71.2	450	16.9	7106	214	16.1	22.29	2.51	0.594
71.2	450	16.9	7205	206	16.1	21.67	2.48	0.585
71.2	450	16.9	7294	199	16.1	20.73	2.40	0.567
71.2	450	16.9	7401	185	16.1	19.27	2.26	0.535
71.2	450	16.9	7499	171	16.1	17.81	2.12	0.501
71.2	450	16.9	7752	136	16.1	14.17	1.74	0.412
71.2	450	16.9	8000	106	16.1	11.04	1.40	0.331
71.2	450	16.9	8251	78	16.1	8.13	1.06	0.251
71.2	450	16.9	8319	70	16.1	7.29	0.96	0.227



Data with Shorter Inlet Nozzles (final configuration)

Measurements					Calculated Results			
Inlet Temp. °F	Inlet Pres. psia	Flow ΔP in. H ₂ O	RPM	Torque readout	Flow rpm	Torque in lb	Net Power Hp	Efficiency
72.0	500	18.5	1254	365	16.9	38.13	0.76	0.154
72.0	500	18.5	1504	360	16.9	37.50	0.89	0.182
72.0	500	18.5	1750	352	16.9	36.77	1.02	0.207
72.0	500	18.5	2002	346	16.9	36.04	1.14	0.233
72.0	500	18.5	2253	341	16.9	35.52	1.27	0.258
72.0	500	18.5	2503	330	16.9	35.00	1.39	0.282
72.1	500	18.5	2752	332	16.9	34.58	1.51	0.307
72.1	500	18.5	3001	328	16.9	34.17	1.63	0.331
72.1	500	18.5	3249	324	16.9	33.75	1.74	0.354
72.1	500	18.5	3502	320	16.9	33.33	1.85	0.376
72.1	500	18.5	3753	316	16.9	32.92	1.96	0.398
72.1	500	18.5	4002	312	16.9	32.50	2.06	0.415
72.1	500	18.5	4249	310	16.9	32.29	2.18	0.442
72.0	500	18.5	4501	306	16.9	31.88	2.28	0.463
72.0	500	18.5	4747	302	16.9	31.46	2.37	0.481
72.0	500	18.5	5002	296	16.9	30.83	2.45	0.497
72.0	500	18.5	5255	291	16.9	30.31	2.53	0.514
72.0	500	18.5	5260	290	16.9	30.21	2.52	0.512
72.0	500	18.5	5503	285	16.9	29.69	2.59	0.527
72.0	500	18.5	5750	281	16.9	29.27	2.67	0.543
72.0	500	18.5	6002	275	16.9	29.06	2.77	0.562
72.0	500	18.6	6256	274	16.9	28.54	2.83	0.574
72.0	500	18.6	6501	271	16.9	28.23	2.91	0.590
72.0	500	18.6	6606	269	16.9	28.02	2.94	0.595
72.0	500	18.6	6700	267	16.9	27.81	2.96	0.599
72.0	500	18.6	6802	266	16.9	27.71	2.99	0.606
72.0	500	18.6	6897	263	16.9	27.40	3.00	0.608
72.0	500	18.6	7001	260	16.9	27.08	3.01	0.610
72.0	500	18.6	7105	258	16.9	26.88	3.03	0.614
72.0	500	18.6	7208	255	16.9	26.56	3.04	0.616
72.0	500	18.6	7300	251	16.9	26.15	3.03	0.614
72.0	500	18.6	7397	244	16.9	25.42	2.98	0.604
72.0	500	18.6	7504	239	16.9	24.90	2.96	0.601
72.0	500	18.6	7750	218	16.9	22.71	2.79	0.566
72.0	500	18.6	8002	179	16.9	18.65	2.37	0.480
72.0	500	18.6	8246	144	16.9	15.00	1.96	0.398
72.0	500	18.6	8505	114	16.9	11.88	1.60	0.325
72.0	500	18.6	8748	84	16.9	8.75	1.21	0.246
72.0	500	18.6	8834	74	16.9	7.71	1.08	0.219

Data with Shorter Inlet Nozzles (final configuration)

Measurements					Calculated Results			
Inlet Temp. °F	Inlet Pres. psia	Flow AP in. H ₂ O	RPM	Torque readout	Flow gpm	Torque in lb	Net Power Hp	Efficiency
67.5	750	27.5	2000	511	20.6	52.21	3.75	0.304
67.5	750	27.5	3071	511	20.6	52.21	3.75	0.305
67.5	750	27.5	3505	506	20.6	52.21	3.75	0.329
67.5	750	27.5	3751	506	20.6	52.29	3.71	0.345
67.5	750	27.5	4007	497	20.6	52.27	3.79	0.365
67.6	750	27.5	4255	492	20.6	52.25	3.66	0.364
67.6	750	27.5	4503	497	20.6	50.75	3.62	0.402
67.6	750	27.5	4753	482	20.6	50.71	3.75	0.420
67.6	750	27.5	5004	477	20.6	49.69	3.55	0.438
67.6	750	27.5	5254	472	20.6	49.17	4.10	0.455
67.6	750	27.5	5504	466	20.6	48.54	4.24	0.471
70.2	750	27.5	5747	460	20.6	47.92	4.27	0.495
70.4	750	27.5	5997	455	20.6	47.40	4.51	0.501
70.5	750	27.5	6251	450	20.6	46.88	4.65	0.516
70.5	750	27.5	6502	445	20.6	46.35	4.78	0.531
70.5	750	27.5	6754	440	20.6	45.83	4.91	0.545
70.5	750	27.5	7006	435	20.6	45.30	5.01	0.557
70.5	750	27.5	7257	430	20.6	44.69	5.14	0.571
70.5	750	27.5	7501	424	20.6	44.17	5.26	0.584
70.5	750	27.5	7755	418	20.6	43.54	5.36	0.595
70.5	750	27.5	8002	412	20.6	42.92	5.46	0.606
70.2	750	27.5	8102	411	20.6	42.81	5.50	0.611
70.2	750	27.5	8200	410	20.6	42.71	5.56	0.617
70.2	750	27.5	8297	406	20.6	42.29	5.57	0.618
70.6	750	27.5	8400	403	20.6	41.98	5.59	0.621
70.6	750	27.5	8501	400	20.6	41.67	5.62	0.624
70.6	750	27.5	8604	396	20.6	41.25	5.63	0.625
70.6	750	27.5	8697	392	20.6	40.83	5.63	0.626
70.6	750	27.5	8804	388	20.6	40.42	5.65	0.627
70.6	750	27.5	8903	384	20.6	40.00	5.65	0.627
70.6	750	27.5	8999	379	20.6	39.48	5.64	0.626
70.6	750	27.5	9101	373	20.6	38.85	5.61	0.623
70.6	750	27.5	9203	366	20.6	38.13	5.57	0.618
70.6	750	27.5	9297	357	20.6	37.19	5.49	0.609
70.6	750	27.5	9500	324	20.6	33.75	5.09	0.565
70.6	750	27.5	9747	278	20.6	28.96	4.48	0.497
70.6	750	27.5	10002	236	20.6	24.58	3.90	0.433
70.6	750	27.5	10249	199	20.6	20.73	3.37	0.374

Data with Shorter Inlet Nozzles (final configuration)

Measurements					Calculated Results			
Inlet Temp. °F	Inlet Pres. psia	Flow in. H ₂ O	RPM	Torque readout	Flow gpm	Torque in lb	Net Power Hp	Efficiency
68.0	900	32.9	4740	559	22.5	61.25	4.50	0.389
68.0	900	32.9	5000	575	22.5	61.77	4.42	0.373
68.0	900	32.9	5250	579	22.5	60.87	4.30	0.474
68.0	900	32.9	5456	576	22.5	59.77	4.20	0.356
68.0	900	32.9	5749	570	22.5	59.17	4.18	0.418
68.0	900	32.9	6000	562	22.5	59.17	4.18	0.418
68.0	900	32.9	6247	555	22.5	57.81	4.05	0.392
68.0	900	32.9	6502	551	22.5	57.81	4.05	0.392
68.0	900	32.9	6760	545	22.5	56.77	3.90	0.373
68.0	900	32.9	7008	538	22.5	56.30	3.85	0.367
68.0	900	32.9	7255	532	22.5	55.84	3.80	0.361
68.0	900	32.9	7512	526	22.5	54.79	3.65	0.346
68.0	900	32.9	7749	520	22.5	54.37	3.60	0.340
68.0	900	32.9	8000	515	22.5	53.65	3.51	0.326
68.0	900	32.9	8249	509	22.5	53.07	3.44	0.318
68.0	900	32.9	8500	504	22.6	52.50	3.39	0.312
68.0	900	32.9	8746	497	22.6	51.77	3.30	0.307
69.0	900	33.0	9000	490	22.6	51.04	3.24	0.301
69.0	900	33.0	9107	486	22.6	50.63	3.20	0.298
70.0	900	33.0	9199	483	22.6	50.31	3.17	0.296
70.0	900	33.0	9311	479	22.6	49.80	3.12	0.292
70.0	900	33.0	9414	475	22.6	49.48	3.09	0.289
70.0	900	33.0	9498	471	22.6	49.17	3.07	0.287
70.0	900	33.0	9606	467	22.6	48.65	3.01	0.281
70.0	900	33.0	9705	462	22.6	48.13	2.97	0.278
70.0	900	33.0	9797	457	22.6	47.60	2.93	0.275
70.0	900	33.0	9900	451	22.6	46.90	2.88	0.271
70.0	900	33.0	9941	443	22.6	46.15	2.82	0.265
70.0	900	33.0	10114	433	22.6	45.10	2.74	0.258
70.0	900	32.9	10199	422	22.5	43.96	2.67	0.251
70.0	900	32.9	10497	363	22.5	37.81	2.30	0.218
70.2	900	32.9	10758	315	22.5	32.81	1.95	0.181
70.1	900	32.9	11003	272	22.5	28.33	1.60	0.150
70.1	900	32.9	4735	588	22.5	61.25	4.50	0.389
70.1	900	32.9	4507	593	22.5	61.77	4.42	0.373
70.1	900	32.9	4247	599	22.5	62.40	4.20	0.356